,

Particulate matter emissions modelling in the context of HFO combustion in large diesel engines

Kristian Hentelä

School of Engineering

Thesis submitted for examination for the degree of Master of Science in Technology.

Espoo 19.9.2016

Thesis supervisor:

Prof. Martti Larmi

Thesis advisor:

D.Sc. (Tech.) Ossi Kaario

Aalto University
School of Engineering

AALTO UNIVERSITY
SCHOOL OF ENGINEERING

ABSTRACT OF THE
MASTER'S THESIS

Author: Kristian Hentelä

Title: Particulate matter emissions modelling in the context of HFO combustion in large diesel engines

Date: 19.9.2016 Language: English Number of pages: 7+55

Department of Energy Technology

Professorship: Ene

Supervisor: Prof. Martti Larmi

Advisor: D.Sc. (Tech.) Ossi Kaario

In the present study a new approach for modelling emissions of coke particles or cenospheres from large diesel engines using HFO was studied. The model is based on a multicomponent droplet mass transfer and properties model developed by V. Garaniya, University of Tasmania, that uses a continuous thermodynamics approach to model the complex composition of the HFO fuel, and the resulting behaviour in regards to fuel properties and mass-transfer processes such as evaporation and pyrolysis. Cenospheres are modelled as the residue left in the fuel droplets towards the end of the simulation. The mass-transfer and fuel properties models were implemented into a cylinder section model based on the Wärtsilä W20 engine in the CFD-code Star CD v.4.24. The different submodels and corresponding parameters were tuned to match experimental data of cylinder pressures available from Wärtsilä for the studied cases.

The results obtained from the present model were compared to experimental results found in the literature. The performance of the model was found to be promising although conclusive validation of the model would require more detailed experimental results about cenosphere emissions from the specific case studied here. According to the results obtained from this model the emissions of cenospheres are a function of both operating conditions and fuel properties. Reducing the share of the heavy residual component in the fuel will decrease these emissions in all conditions and thus switching to better quality fuels, with less residue, should decrease these emissions. Reducing the emissions is also possible through changing operating conditions. Improving the burnout of the carbonaceous particles decreases emissions and thus increasing the load or improving atomization leads to lower emissions.

Keywords: HFO, Cenospheres, CFD-modelling, Particulate matter, Emissions, Diesel engine

AALTO-YLIOPISTO
INSINÖÖRITIETEIDEN KORKEAKOULU

DIPLOMITYÖN
TIIVISTELMÄ

Tekijä: Kristian Hentelä

Työn nimi: Hiukkaspäästö mallinnus raskasta polttoöljyä käyttävistä suurista diesel moottoreista

Päivämäärä: 19.9.2016 Kieli: Englanti Sivumäärä: 7+55

Energiatekniikan laitos

Professuuri: Ene

Työn valvoja: Prof. Martti Larmi

Työn ohjaaja: D.Sc. (Tech.) Ossi Kaario

Tässä työssä tutkitaan uutta lähestymistapaa koksi hiukkasten, tai niin kutsuttujen cenospherien, päästöjen mallintamiseen raskasta polttoöljyä käyttävistä suurista diesel moottoreista. Käytetty malli perustuu V. Garaniyan University of Tasmaniassa kehittämään multikomponentti-pisaran massansiirto- ja ominaisuusmalliin. Malli käyttää jatkuvan termodynamiikan lähestymistapaa mallintaakseen raskaan polttoöljyn monimutkaista koostumusta ja siitä johtuvia polttoaineen ominaisuuksia. Täten voidaan mallintaa polttoainepisairoiden höyrystymistä ja pyrolyysiä huomioiden pisaran koostumus. Cenospherejä mallinnetaan tarkastelemalla pisaroihin jäljelle jäävää massaa kun höyrystymis ja pyrolyysi prosessit ovat pysähtyneet simulaation lopussa. Massansiirto- ja pisaran ominaisuusmallit implemetoitiin Wärtsilän W20 moottoriin perustuvaan sylinteri sektori malliin Star CD v.4.24 CFD ohjelmassa. Eri alimallit ja niiden parametrit säädettiin siten, että simulaatiotulokset vastasivat mahdollisimman hyvin koetuloksia mitattujen sylinteripaineiden suhteen.

Mallista saatuja hiukkaspäästö tuloksia verrattiin kirjallisuudesta löytyviin kokeellisiin tuloksiin. Mallin suorituskyky todettiin lupaavaksi, vaikka mallin perusteellinen validointi vaatisi yksityiskohtaisempia kokeellisia tuloksia liittyen cenospherien tuotantoon tutkitussa prosessissa. Tämän työn tulokset näyttävät että cenosphere päästöt ovat sekä prosessin olosuhteiden että polttoaineen ominaisuuksien funktio. Polttoaineen raskaimpien komponenttien osuuden vähentäminen vähentää näitä päästöjä kaikissa olosuhteissa, ja siten parempilaatuisen polttoaineen käyttämisen pitäisi johtaa näiden päästöjen vähenemiseen. Päästöjä on myös mahdollista vähentää muuttamalla prosessin olosuhteita. Hiukkasten palamisen parantaminen vähentää pääsöjä, ja siten kuorman lisääminen tai polttoainesuihkun atomisaation parantaminen johtaa alhaisempiin pääsöihin.

Avainsanat: Hiukkaspäästöt, raskas polttoöljy,CFD mallinnus, Diesel moottori

Contents

Symbols and abbreviations

Symbols

T_D	Droplet temperature
T_{cr}	Critical temperature
T_{REF}	Reference temperature
R	droplet radius
θ_{Lj}	Mean molecular weight of component j
θ_{jR}	Mean molecular weigth of component j at the surface of the droplet
σ^2_{Lj}	Variance of the molecular weight of component j in the liquid phase
σ^2_{jR}	Variance of the molecular weight of component j at the surface of the droplet
γ_j	Distribution origin for the distribution of the molecular weight of component j
ψ_{Lj}	second central moment of the distribution of molecular weight of component j
ψ_{jR}	second central moment of the distribution of molecular weight of component j at droplet surface
α_{Lj}	Shape parameter for distribution for molecular weight of component j in the liquid phase
β_{Lj}	shape parameter for distribution for molecular weight of component j in the liquid phase
y_{FjR}	Concentration of fuel vapour from component j at droplet surface
$y_{Fj\infty}$	Concentration of fuel vapour from component j in surrounding medium, has a value of 0 in this model
R_{GC}	Universal gas constants
P_{atm}	Atmospheric pressure
P_∞	Pressure in the surrounding medium
N	Total molar flux of fuel vapour from droplet surface
ξ_j	Molar flux fraction of component j
Sh_0	Sherwood number for stationary droplet, = 2 in this model
S_{fgj}	Enthropy of evaporation for component j
D_j	Diffusivity of component j
AR	Aromaticity
B_j	Mass transfer number
E_1	Activation energy
k_1	Pre-exponential factor for reaction rate
E_2	Activation energy
k_2	Pre-exponential factor for reaction rate
E_3	Activation energy
k_3	Pre-exponential factor for reaction rate
E_{poly}	Activation energy
A_{poly}	Pre-exponential factor for polymer
K_c	Chemical rate coefficient
K_d	Diffusion rate coefficient
C_{pLj}	Specific heat of liquid for component j
c	molar density

τ_C	Characteristic time
τ_{ch}	Chemical time-scale
τ_ϵ	Turbulent mixing time-scale
f_{delay}	Delay function in LaTCT model
W_l	Chemically limited reaction rate
W_t	Turbulent mixing limited reaction rate
r	stoichiometric fuel to oxygen ratio in LaTCT model
We	Weber number
Re	Reynolds number

Operators

$\frac{\mathrm{d}}{\mathrm{d}t}$	derivative with respect to variable t

Abbreviations

HFO	Heavy Fuel Oil
PM	Particulate matter
CFD	Computational fluid dynamics
IFO	Intermediate Fuel Oil
LCO	Light cycle oil
HCO	Heavy cycle oil
CFI	Coke Formation Index
LAC	Light absorbing carbon
PDF	Probability Density Function
VLE	Vapour-Liquid Equilibrium
LaTCT	Laminar and Turbulent Characteristic time combustion model
FSN	Filter Smoke Number
SMD	Sauter Mean Diameter

1 Introduction

Despite ever tightening restrictions on emissions and emerging alternative fuels, Heavy Fuel Oil (HFO) will still remain an important fuel for the foreseeable future, especially within the maritime transport industry[1], [2]. While the market share of HFO might decrease over time, from about 80 % in 2010 due to the emergence of alternative fuels, Lloyds Register Marine still forecasts the share of HFO in the marine fuel market in 2030 to be between 47 % and 66 %.[1] With the increase in fuel demand this means that the total consumption of HFO is actually likely to increase in the near future.

The term HFO usually refers to the heaviest fuel that is produced from crude oil. It consists mostly of the residue that remains once all the lighter fractions have been extracted from the crude oil during the refining process, although some amount of lighter fractions are added to it as cutter stock in order to achieve desired values for fuel characteristics such as viscosity and sulphur content[3]. This means that HFO contains a large amount of different hydrocarbons ranging from lighter molecules such as paraffins and naphthenes to very heavy molecules such as asphaltenes[3]. As HFO is derived from the residue of the refining process, its properties will actually differ according to the refining process used. As the crude oil refining process has been developed over the years in order to produce ever larger shares of valuable distillate fuels the quality of HFO has deteriorated. When all lighter fractions are removed only the heaviest fractions and impurities remain in the residue used to make HFO. The result is a fuel with high asphaltene content which may lead to issues when it is used in marine diesel engines. The high asphaltene content can cause problems with poor ignition and combustion. Additionally it increases the production of carbonaceous particles in the combustion process which leads to both increased particulate emissions and possible fouling of engine components.[3]

This continuing prevalence of HFO as a transport fuel coupled with tightening environmental regulations means that there will be a demand for emissions abatement solutions for HFO combustion processes [2]. Additionally optimization of HFO combustion process is also useful for minimizing the challenges presented by using heavy fuels in large diesel engines. One challenge presented by using heavy fuel in an engine is the different behaviour with regards to emissions of particulate matter(PM) compared to operation with lighter fuels. PM emissions modelling in diesel combustion processes is generally focused on modelling soot particles formed in gas phase reactions between fuel molecules. Although this may give an accurate estimate when modelling emissions from operation with light distillate fuels, in combustion of HFO other mechanisms of PM formation are prevalent and gas phase soot presents only a fraction of total PM. The larger amount of impurities in HFO leads to larger emissions of ash and sulphates. In addition to this, the poorly evaporating heavy molecules present in HFO can lead to the formation of carbonaceous residue directly from the fuel droplets. While the ash emissions are easily estimated from the ash content in the fuel, predicting the emissions of the carbonaceous particles formed

from the fuel droplets, commonly referred to as cenospheres, is more complicated.

The purpose of this thesis is to model and study the formation of carbonaceous particles from the fuel droplets in HFO combustion in a diesel engine. In order to achieve this a multi-component droplet evaporation model by Garaniya [3] is implemented into a CFD model based on the Wärtsilä W20 engine. The Star-CD v4.24 CFD software is used to run the simulations. The droplet evaporation model uses continuous thermodynamics in order to model the complex composition of HFO and contains a model for the formation and consumption of carbonaceous residue in the fuel droplet. This is then used to model the emissions of particulate matter from the engine. Through modelling the emissions of PM this thesis hopes to provide a tool for predicting PM emissions from HFO combustion as well as providing insight into the formation of these emissions. Understanding the mechanisms of formation and consumption of PM emissions is essential when developing engines in order to diminish these emissions.

2 Background

In order to understand the reasoning behind the present model it is useful to have some basic understanding of both the fuel modelled here, HFO, and the challenges it presents when it comes to modelling particulate emissions. It is for instance crucial to understand and differentiate between different types of particles emitted from the HFO combustion process in order to be able to correctly interpret the results provided by the present model when comparing them to experimental data. Therefore this section will include background information about HFO in general and particles formed in HFO combustion. Additionally the problems arising from emissions of particulate matter are shortly presented in order to highlight the importance of research into the area. Finally soot and particulate modelling approaches found in literature are presented and evaluated in order to give an overview of the state of research into this topic at the moment.

2.1 Heavy Fuel Oil

Heavy fuel oil as a term describes quite a wide range of different fuels and it is therefore hard to give an exact definition of HFO. Simply defining it as the the residue of the crude oil refining process is not accurate as lighter fuel oils are often added to the residue in order to produce a fuel with required properties. These blends are sometimes referred to as Intermediate fuel oils (IFO). However IFO:s with a significant share of residue are still commonly categorized as heavy fuel oil [4]. To be clear it is therefore useful to define HFO in terms of its properties. In Annex I of the Marpol convention Heavy fuel oil is defined as having a density at 15°C of more than 900 kg/m^3 or a kinematic viscosity at 50°C of more than 180 mm^2/s[5]. The ISO 8217 standard divides marine fuels into distillate and residual fuels. The residual fuels referred to in ISO 8217 provide perhaps the most useful definition of HFO for use in engines as the standard was developed to meet the requirements of use onboard ships.[6] The residual fuels specified in ISO 8217 have kinematic viscosities at 50°C ranging from 30 mm^2/s to 700 mm^2/s, and densities of 960-1010 kg/m^3[7]. The sulphur content of the fuel directly corresponds to SO_x emissions from its combustion. Therefore efforts to limit emissions of sulphur oxides have led to limits on the allowed sulphur contents in fuels. In Annex of Marpol 73/78, which was adopted in 2008, limits the sulphur content of all marine fuels to 3.5 %. For fuel used within emissions control areas (ECA) the sulphur content of the fuel is further limited to 0.1 % since 2015.[7]
As the maritime shipping industry only makes up a small fraction of the market for petroleum based fuels, its needs do not dictate the terms for the crude oil refinery processes utilized globally[8]. This means that the trend is to strive for ever higher distillate yields from crude oil refining, which in turn leads to lower quality of the residue that is used for HFO[8]. The main processes used in crude oil refining are:

- Atmospheric distillation

- Vacuum distillation
- Visbreaking
- Catalytic cracking

Each of these processes, beginning with atmospheric distillation, is aimed at extracting more valuable distillate fuels from the crude oil feedstock. In atmospheric distillation crude oil is simply boiled at temperatures up to 371°C and the different products are condensed and collected at different heights in a fractionating tower. The residue from this process was in the past used as HFO and these straight run residual fuels were of good quality with regards to both combustion characteristics and handling.[8]

By introducing a partial vacuum to the atmospheric distillation process, additional distillates can be extracted from the residue. This however further concentrates impurities and heavy molecules in the residue and the resulting properties such as very high viscosity make the residue difficult to use as a fuel as such. The residue is therefore used as feedstock in a viscosity breaking process which reduces the viscosity of the feedstock using a mild form of thermal cracking. Visbreaking yields a residue that has some unfavourable properties, such as high asphaltene content, compared to the straight run residue of the atmospheric distillation process.[8]
The catalytic cracking process uses a catalysed version of thermal cracking in order to convert the heavy distillate from the vacuum distillation into lighter molecules.[7] This process is used to further increase the yield of light hydrocarbons from the refining process. In addition to increasing the gasoline yield of the process catalytic cracking also produces light cycle oil, LCO, and heavy cycle oil, HCO, which are amongst other things used for HFO blending.[7]

As the crude oil refining industry has strived for higher yields of lighter cuts, and began to utilize crude oils of lesser quality, the quality of the resulting residue has deteriorated[8]. Therefore in order to increase the value of this residue some fraction of lighter distillate cuts are added to the residue as cutter stock.[8] The resulting fuel may have the desired qualities when it comes to viscosity and sulphur content and other such properties. It also however consists of a very wide range of different hydrocarbons. Heavy molecules, such as asphaltenes, are concentrated in the residue and the cutter stock consists of significantly lighter molecules. This kind of a composition could be problematic when modelling the behaviour of the fuel and, therefore, a model that takes the composition into account could shed light on some of the phenomena encountered in HFO combustion.

2.2 Particulate formation in HFO combustion

In this section the formation of particulate matter in combustion processes is examined. The term particulate matter can actually refer to a range of different emissions stemming from different mechanisms in the combustion process. It is therefore of high importance to identify and differentiate between the different mechanisms of PM formation when attempting to model these emissions. The proposed model in this study does not attempt to model the complete range of PM emitted from HFO combustion but only attempts to model one specific kind of PM emitted from this process, cenospheres. Cenospheres, which are often also referred to in literature as coke or char particles, are the particles that are left behind by incomplete evaporation and combustion of fuel droplets. This is important to keep in mind when comparing simulation results with experimental data.

The mechanisms involved in the formation of particulate matter are essentially the same in most fossil fuel combustion processes, but the fuel and the combustion process used determine which of these mechanisms are most important. Essentially the particles formed in combustion processes can be divided into two distinct categories. The first category is ash which constitutes from the non-organic elements present in the fuel, and the second category is carbonaceous particles which results from incomplete combustion of the fuel. Further the carbonaceous category can be divided into larger char or coke particles that form directly from the fuel droplets and soot particles which are formed by gas phase reactions of evaporated fuel. In addition to the primary particles formed in the combustion process, particles are also formed as compounds, mainly SO_x, in the exhaust gas react with the ambient atmosphere after exiting the combustion chamber. The amount of these kinds of secondary particles formed in the exhaust gas can be quite significant in fuels containing large amounts of sulphur.[9]

In HFO combustion much of the inorganic compounds in the fuel will evaporate and form particles through nucleation. The nucleation mode particles are very small and this means that the primary ash particles may have diameters of only 0.04—0.1 μm[10]. Evaporated fuel molecules can also form particles as they go through chemical reactions in the gas phase. The small particles thus nucleated from the gas phase are what is commonly referred to as soot. These soot particles have diameters of around 10-80 nm and consist to a large part of elemental carbon[11]. Soot particles dominate PM emissions in smaller diesel engines operating on lighter fuels but are also present in HFO combustion in larger engines, although the high fuel to air ratio in such engines promote the oxidation of soot thus reducing emissions[11]. Although the nucleated soot and ash particles in HFO combustion are very small they can stick together forming agglomerates with sizes of up to a few microns.
The PM formation mechanism which is modelled by the present model is coke particle formation from the fuel droplets in the liquid phase. In combustion of lighter fuels such emissions are not an issue as the fuel evaporates more or less completely. Due to the presence of heavy molecules originating from the residue portion of the HFO, the evaporation behaviour of HFO is more complex and the

prospect of formation of particles from the liquid phase needs to be considered. In order to understand the formation of a coke particle from the HFO droplet one needs to understand the different stages involved in the combustion of a HFO droplet.

According to Ikegami et al.[12] the combustion process of a HFO droplet consists of two distinct phases, a liquid droplet phase and a solid coke particle phase. First comes the liquid droplet phase where the droplet turns into a solid coke particle through various heat- and mass-transfer processes. This phase can be seen as comprising of the following four stages:

- Pre-ignition heating
- Evaporation
- Thermal decomposition
- Polymerisation

In short the droplet first heats up leading to the evaporation of lighter components in the droplet in order of their volatility. As the temperature rises high, enough thermal cracking starts to take place and heavy molecules brake down into lighter compounds which then evaporate. Lastly a process of polymerisation starts to take place, combining lighter molecules into polymer and thus solidifying the droplet into a coke particle. This begins the solid coke particle phase where the coke particle formed in the previous phase burns through surface oxidation. Essentially every fuel droplet will become a coke particle that is then consumed through surface oxidation[13].
While a considerable part of combustion modelling studies have focused on modelling distillate fuels there have also been attempts to model the complex behaviour of HFO described above. Most notably in this context Garaniya proposed the model that is implemented into diesel combustion and emissions modelling in this study.[3] Garaniyas work was influenced partly by the work of Baert, who proposed a droplet evaporation and pyrolysis model using four components to represent the composition of HFO[14]. While the evaporation modelling in Garaniyas model is different from Baert's, the droplet pyrolysis and polymerisation model was modified from the pyrolysis model of Baert.
Goldsworthy [15]has developed a HFO combustion and ignition model in the context of marine diesel engines. Goldsworthy used two components, cutter stock and residue, to model the properties of HFO[15]. Goldsworthys' model is however not suited for modelling coke particle emissions as the formation of carbonaceous residue in the droplets is not modelled apart from raising the critical temperature of the droplet to allow it to stay in the simulation. Struckmeier[16] elaborated on Goldsworthys work adding a two component evaporation model, and Kyriakides[17] also developed a HFO model based on a similar two component approximation of the fuel. These models also do not however address the issue of coke formation in the liquid phase.

The coke particles produced in HFO combustion will, given the right conditions, eventually be consumed completely. However, if there is not sufficient oxygen or

time for this they will exit the process as PM emissions. High aromatic content in the fuel seems to be correlated with coke or cenosphere formation and cenosphere emissions are associated with fuels with high asphaltene contents[3], [18]. However, predicting cenosphere emissions based on fuel properties alone seems problematic as there are studies contradicting direct correlations between asphaltene content and cenosphere emissions[13], [19]. Marrone et. al found coke formation even with fuels where asphaltenes had been removed, and thus prediction of coke formation purely based on asphaltene content is problematic[19]. Therefore the modelling approach used in this study could provide useful information on conditions leading to cenosphere emissions.

2.3 Modelling Particulate Matter in litterature

Soot models can roughly be divided into three different categories, empirical models, semi-empirical models and detailed theoretical models. In empirical models equations are adjusted in order to reproduce correlations observed in experimental data. Empirical models can provide reliable predictions for the case for which they were created. They are also often fairly simple and require relatively little computational resources. They do not, however, necessarily take into account any of the physical processes involved in soot formation or consumption and are therefore not directly applicable for cases with very different conditions.[20]
The polar opposite of purely empirical models are detailed theoretical models which attempt to describe the formation and consumption of soot particles from first principles. As they are based on physical principles, working theoretical models should be applicable to a wide variety of cases. Due to the fact that the production of soot emissions is such a complicated process, creating a model that incorporates all the different chemical and physical processes involved is very difficult. In addition such a model would require significant amounts of computational power, and thus creating and using detailed theoretical models may not always be practical.[20]
Semi-empirical models are a compromise between the two extremes represented by purely empirical and theoretical models. Semi-empirical models often use rate equations that are simplifications of the actual physical processes involved where the parameters of the equations are set according to experimental data to ensure accuracy. The simplifications can be either due to a need to save computational time or avoiding the need to model a phenomena that might not be well enough understood. As semi-empirical models do still have a connection to the actual physical processes involved they can provide more reliable predictions than purely empirical models when multiple operating conditions are changed[20]. As the present model attempts to model the formation of cenospheres from first principles it could be considered a detailed theoretical model.

The modelling of PM emissions from diesel engines seems to be very concentrated on modelling the formation and consumption of soot in the gas phase and a multitude of different models exist for this purpose[20]. As the present model is focused on modelling the coke particles formed directly from the fuel droplets it is essentially

a completely different thing and therefore a summary of gas phase soot models in the literature would not be useful for the purposes of this study. It however proved difficult to find any applications of modelling of cenosphere emissions in the context of internal combustion engines. In fact, no detailed studies were found on the matter in the context of diesel engines. Some models for the formation of cenospheres or coke particles were, however, found even though they were mostly developed for use with HFO fired boilers. Baert studied the relation of droplet size, asphaltene content and coke formation with an approach similar to the one used in this work[14]. The results of that study showed that reducing the droplet size would seem to be an effective way to reduce coke emissions[14].

Additional approaches to modelling cenosphere formation were developed by Antaki[21], Lee et al.[22], Moszkowicz et al.[23] and Youan et al.[24]. The models of Antaki, Lee and Moszkowicz all assume that cenospheres are hollow spheres with a shell of coke. In all these models the formation of the hollow sphere is modelled by assuming that the coke formed as residue of the combustion process is gathered at the surface of the droplet forming a rigid porous shell. The liquid then evaporates through the shell thus thickening the shell and finally leaving the sphere hollow. In Antakis' model the droplet is assumed to form a cenosphere with the same size as the original droplet, while in the models of Lee and Moszkowicz the size of the cenosphere is governed by a critical shell thickness[25]. The most recent model found in the literature was developed by Reddy et al. [25]. In the model of Reddy et al. the formation of cenospheres is modelled in three stages; regression, shell formation and hardening and flow through rigid shell. In contrast to the models of Lee and Moszkowicz the size of the resulting cenospheres is not governed by an assumed critical value for shell thickness. Instead the critical value of cenosphere diameter is modelled through the balance of the pressures created by vapour flowing through the shell and the pressure on the shell due to the van der Walls energy of the coke layers and the surface energy[25]. One problem with implementing models such as the one by Reddy et al. for modelling in medium speed diesel engines is that the model was validated for quite large droplet sizes. The model of Reddy et al. was validated against experimental data for droplets with sizes of 490, 640 and 690 μm[25]. These droplet sizes are quite large compared to those observed in spray studies for HFO in marine diesel engines[26].

According to Youan et al. the assumption of large hollow spheres works for sprays where the fuel droplets are large, but used instead an assumption of uniform density in the cenospheres as it was deemed more appropriate for sprays with smaller droplets[24]. Urban et al. found that the amount of a given fuel oil that is converted into cenospheres is mainly a function of fuel properties and fairly constant over a range of different operating conditions. They developed a measure for this called the CFI (Coke Formation Index) and speculated that it could be used to predict coke production in cases where droplet size distributions in the spray and the CFI of the fuel are known[27]. The CFI is essentially a simple empirical approach to modelling coke formation.

2.4 Effects of PM emissions

The combustion process produces a variety of different kinds of particles as described in previous sections and each of these types of particles has a different effect both on the equipment used in the combustion process and the surrounding environment. Particles have different effects on human health both depending on their size and their chemical composition. PM emissions from HFO simultaneously contribute to global warming, through for instance deposition of light absorbing carbon(LAC) on polar icecaps, and cause cooling of the atmosphere through increased cloud formation. It is therefore useful to have some understanding about the effects of particles in order to be able to understand the benefits or problems that changes in these emissions can bring.

As global warming has become a global issue, studying the effect of aerosols on the climate in addition to greenhouse gases has become of interest. Carbonaceous particles absorb light and thus increase the warming of the atmosphere. These particles are often referred to as Black Carbon or by the slightly broader term Light absorbing carbon[28]. However other types of particles such as sulphite particles commonly found in HFO exhaust have the opposite effect on the climate and the total effect on the climate depends on the balance between these two effects. Especially when using HFO with high sulphur content the total effect on the climate tends to be cooling of the climate.[28]
One of the biggest issues associated with emissions of PM is their potential impact on human health. In order to affect human health the PM has to be able to enter the body. Therefore most health effects are associated with smaller particles.[29] When assessing the effect of particulates on human health the focus is therefore often on particles smaller than 10 μm, commonly denoted as PM_{10}. As even smaller particles can have different effects in humans the effects of particles smaller than 2.5 μm or $PM_{2.5}$ are also studied[29]. Since PM_{10} by definition includes also a fraction of $PM_{2.5}$ it is, however, somewhat difficult to disentangle the effects of these[30]. When these kinds of particles are inhaled they can cause respiratory diseases and lung cancer and even enter the bloodstream and cause cardiovascular diseases[29]. In addition to the size of the particles also the chemical composition of the particles affect their effect on humans. For instance the transition metals found in HFO exhaust can increase the toxicity of particles[31].

3 Research material and methods

The present study is based on the droplet evaporation and droplet properties models developed by Garaniya[3] and presented in his thesis titled "Modelling of Heavy Fuel Oil Combustion using Continuous Thermodynamics".[3] The model was developed to be used with the CFD-program Star-CD and is implemented into Star-CD with user subroutines using Fortran coding. The two main user subroutines that are used to implement the model are the subroutines drmast.f and dropro.f found in Star CD. These subroutines allow the specification of custom mass-transfer processes for droplets and droplet properties. The model was originally developed for Star-CD v3.24 but the subroutines were updated in order to be compatible with the newer v4.24 which was used in the present study.
In the following sections the model and the theory behind it are described. Details about its implementation into the Star-CD CFD code are also given along with an explanation about how the model can be applied to PM emissions modelling. Since there are many other submodels involved in the complete combustion model the choises of the most important submodels and the settings for these models in Star CD are also presented in order to give a complete understanding about the whole CFD model used for this work.

3.1 The present model

The idea behind the present model is to use continuous thermodynamics in order to represent the complex composition of HFO. This allows the model to consider the composition of the fuel when calculating the mass-transfer processes from the fuel droplets, without using excessive amounts of computational resources.
As discussed in earlier sections HFO contains such a large range of different hydrocarbons with varying structures and molecular weights, that modelling each of them as discrete components would not be practical.[3] Garaniyas droplet evaporation model solves this issue by using continuous thermodynamics to describe the composition instead of attempting to model each individual component in the fuel. This reduces the computational load while still managing to capture the behaviour of complex fuels. In continuous thermodynamics the fuel mixture composition is represented using Probability Density Functions(PDF) of a characterizing variable. This characterizing variable is then used to predict other properties of the component. In the present model the molecular weight of the components is chosen as the characterizing variable, and the changes in other properties is modelled according to the change in the molecular weights of the components. In the present model the composition of the fuel is described by using four different components, each of which uses a PDF to describe a range of similar hydrocarbons. Three of the components describe lighter components in HFO that originate mainly from the cutter stock and the final component describes the heavy molecules that come from the fraction of heavy Residue in the fuel. The components used in this model are:

- N-Paraffins

- Aromatics
- Naphtenes
- Residue

The distribution of the molecular weights within these components is described using a distribution function. In the present model a Γ-distribution function(Schultz or Pearson type III function) is used. The Γ-distribution can be given as

$$F_j(I) = \frac{(I-\gamma_j)^{\alpha_j-1}}{\beta_j^{\alpha_j}\Gamma(\alpha_j)} \exp(-(\frac{I-\gamma_j}{\beta_j})) \tag{1}$$

where I is the characterizing variable, α_j and β_j, are shape parameters for the function and γ_j is the distribution origin. Both α_j and β_j in this model are different for the liquid phase and the vapour phase while γ_j is assumed to be the same in both phases. The mean and variance of this distribution for the liquid phase are given as

$$\theta_{Lj} = \alpha_{Lj}\beta_{Lj} + \gamma_j \tag{2}$$

$$\sigma_{Lj}^2 = \alpha_{Lj}\beta_{Lj}^2 \tag{3}$$

where θ_{Lj} is the mean and σ_{Lj}^2 is the variance. The distribution parameters used for the different components in the beginning of the simulation are summarized in table 1. The shape of the distributions corresponding to the distribution parameters in

Table 1: Distribution parameters for Γ distribution

Components	Distribution Origin (γ)	Distribution mean (θ)	Standard deviation (σ)
1. n-Paraffins	160	340.00	43.69
2. Aromatics	160	300.00	45.75
3. Naphtenes	160	370.00	45.47
4. Residue	500	850.00	320.15

Table 1 are presented in Figure 1. As the droplets are injected into the cylinder they will undergo mass-transfer processes and the distribution parameters change during the simulation to account for the fact that the lightest components within each of the four fractions evaporate first. In the present model the mass transfer from the three lighter fractions is assumed to happen only through evaporation and the residue fraction is assumed not to evaporate, but to go through pyrolysis instead. After pyrolysis is complete, the pyrolysis residue will burn through heterogeneous surface oxidation. The mass transfer processes modelled in the present model are illustrated in figure 2. In the following subsections explanations for how the different processes illustrated in figure 2 are modelled with the present model. In order to keep the explanation of the model clear and concise the derivation of some equations is not explained in detail. For detailed theoretical explanations about the model readers should consult the original work by Garaniya on the development of the model.[3]

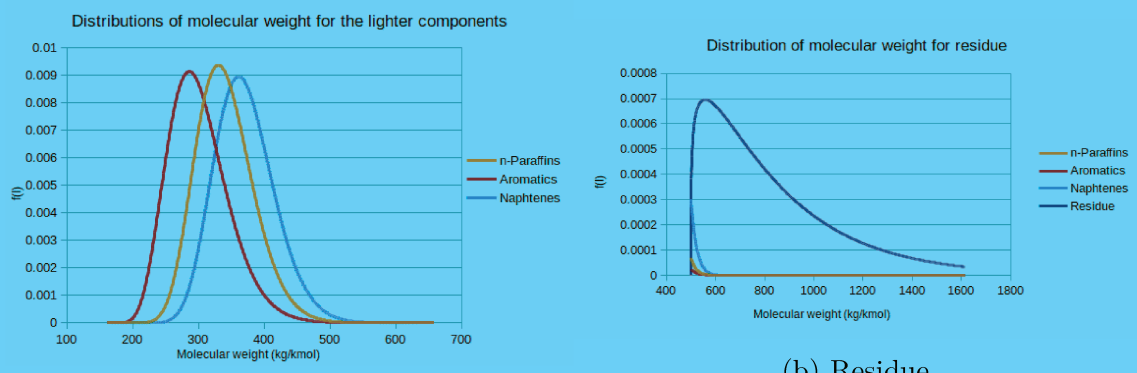

(a) Lighter components

(b) Residue

Figure 1: The PDF:s of the molecular weights of the different components at the beginning of simulations

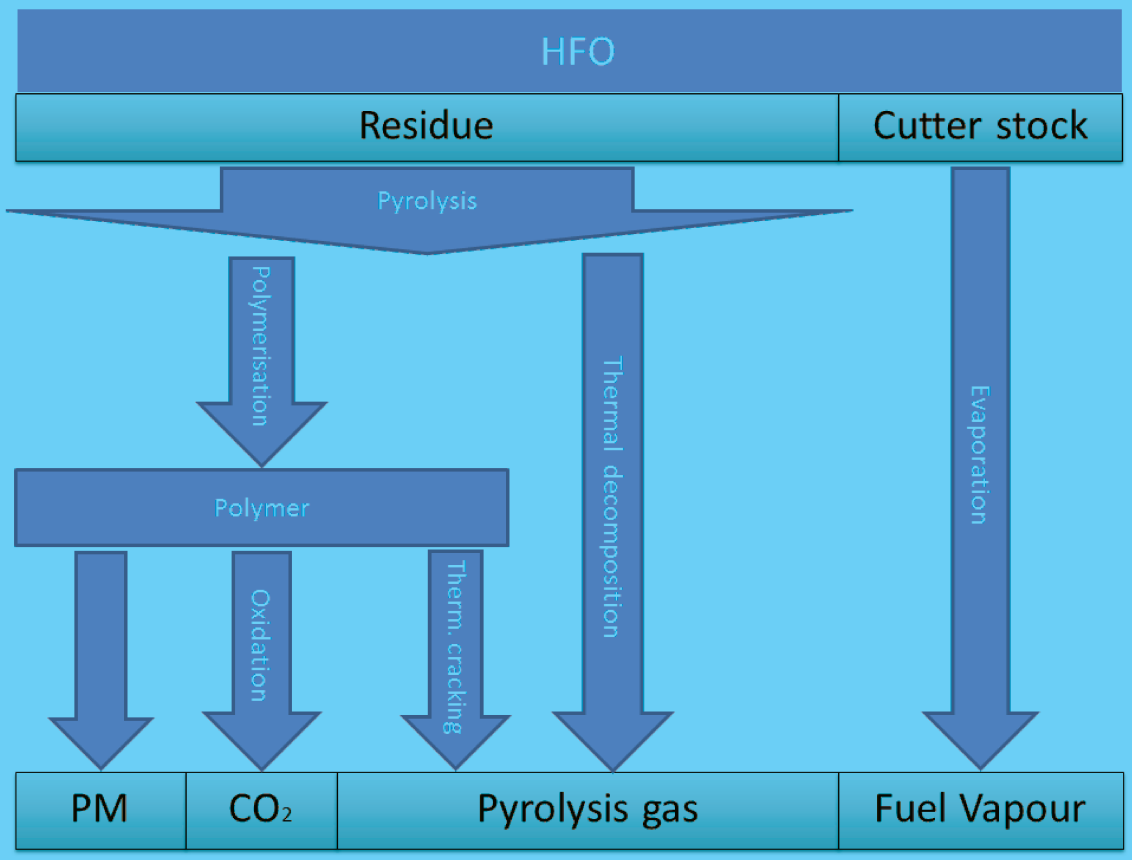

Figure 2: The mass-transfer processes modelled in the present model

3.1.1 Evaporation

Evaporation from the droplet surface is modelled through determining the Vapour-Liquid Equilibrium (VLE) at the droplets surface. As the VLE determines the concentration of vapour at the droplet surface it can be used to determine the evaporation of a component from the surface. The formulation of the VLE stems

from the assumption that the chemical potential μ is the same for each phase at the boundary between phases. This can be stated as[3]

$$\mu_i^G = \mu_i^L \quad \text{for} \quad i = 1, 2, 3...s \tag{4}$$

where s is the total number of species. To describe the evaporation of a fuel consisting of such a large number of species as HFO would then include solving a huge number of chemical potential equations. Here continuous thermodynamics can significantly lower computational cost as an equation only needs to be solved for each component class, of which there are only four in the present model. The VLE formulation used in the present model is the low-pressure VLE model used by Garaniya [3]. This formulation makes the assumption that the vapour phase can be approximated as an ideal gas. The VLE can then be expressed using Raoult's law and formulated for component j using continuous thermodynamics as

$$y_{Fj}\, f_{Vj}(I)\, P = x_{Lj}\, f_{Lj}(I)\, P_j^{sat}(T, I) \tag{5}$$

where y_{Fj} is the vapour phase mole fraction of component j, x_{Lj} is the liquid phase mole fraction of component j, $f_{Lj}(I)$ and $f_{Vj}(I)$ are the liquid and vapour phase distributions for the molecular weight and $P_j^{sat}(T, I)$ is the vapour pressure of the component. The correlation in eq.5 can be used to solve the vapour phase mole fraction at the droplets surface $y_{FjR}$and the distribution parameters, mean molecular weight Θ_{jR} and variance σ_{jR}^2, describing the fractions composition. Using the Clausius-Cleyperon equation to determine the vapour pressure of the component y_{FjR}, Θ_{jR} and σ_{jR}^2 are given as

$$y_{FjR} = \frac{\frac{P_{atm}}{P_\infty} \cdot \exp((\frac{S_{fgj}}{R_{GC}T_R})(T_R - a_B - \gamma_j b_B))}{(1 + \frac{S_{fjg}}{R_{GC}T_R} b_B \beta_{Lj})^{(\alpha_{Lj})}} \tag{6}$$

$$\theta_{jR} = \gamma_j + \frac{\theta_{Lj} - \gamma_j}{1 + ((\frac{S_{fgj} b_b}{R_{GC}T_R} \frac{\sigma_{Lj}^2}{\theta_{Lj} - \gamma_j}))} \tag{7}$$

and,

$$\sigma_{jR}^2 = \sigma_{Lj}^2 (\frac{\theta_{jR} - \gamma_j}{\theta_{Lj} - \gamma_j})^2 \tag{8}$$

The total molar flux of vapour from the droplet is denoted as N. This is the sum of the molar fluxes caused by each of the components and ξ_j is the share of N that is caused by a single component. The ξ_j:s of each component are calculated as

$$\xi_j = \frac{y_{FjR} - y_{Fj\infty}}{\exp(2NR/cD_j Sh_0) - 1} \tag{9}$$

where c is the molar density, D_j is the average diffusivity of the component and $y_{Fj\infty}$ is the vapour phase mole fraction of component j far from the droplet. Sh_0 in eq. 9 is the sherwood number and it is given as a constant $Sh_0 = 2$ as the droplet is stationary during the calculation of a single droplet. The total molar flux N and the

molar flux fractions for each component have to be solved simultaneously to calculate the value of ξ_j and N. As species with light molecular weight evaporate first and leave the liquid phase, the distribution of molecular weights for each component changes. The mean molecular weight increases and the variance decreases. As component j evaporates with a fraction ξ_j of the total molar flux N the corresponding change of mean molecular weight is

$$d\theta_{Lj} = \frac{dt \cdot 3N}{x_{Lj}\, c_L\, R}(\theta_{Lj}\xi_j + \frac{\theta_{j\infty}\, y_{Fj\infty} - \theta_{jR}\, y_{Fjr}(1 + B_j)}{B_j}) \tag{10}$$

The change in the second central moment of the distribution $\psi_{Lj} = \theta_{Lj}^2 + \sigma_{Lj}^2$ can be calculated as

$$d\psi_{Lj} = \frac{dt \cdot 3N}{x_{Lj}\, c_L\, R}(\psi_{Lj}\xi_j + \frac{\psi_{j\infty}\, y_{Fj\infty} - \psi_{jR}\, y_{Fjr}(1 + B_j)}{B_j}) \tag{11}$$

B_j in equations 10 and 11 is given as

$$B_j = \frac{y_{FjR} - y_{Fj\infty}}{\xi_j - y_{FjR}} \tag{12}$$

The rate of evaporation of each component is then given as

$$\frac{dm_{Vj}}{dt} = -N\xi_j A\theta_{jR} \tag{13}$$

where A is the surface area of the droplet.

3.1.2 Pyrolysis

As stated earlier the Residue component is assumed not to evaporate in the present model. The mass transfer processes from this component are assumed to happen only through pyrolysis. The processes involved in the pyrolysis of the residue fraction of the fuel, and modelled in the present work, are presented in Figure 2. The chemical bonds in the heavy molecules are broken due to the influence of high temperatures producing radicals. These radicals then either decompose and become lower molecular weight gases, or recombine through polymerisation producing coke residue. Polymerisation and thermal cracking occur simultaneously and non-aromatic part of formed polymer can also decompose through cracking. Thus both the thermal cracking and polymerisation have a dependence on both temperature and the aromaticity of the fuel (AR).[3]
The pyrolysis model in the present work is based on the work of Baert with modifications to some model parameters[14]. The rate of pyrolysis gas production from the thermal cracking of liquid and polymer is given as

$$\frac{dm_G}{dt} = (m_{component} + m_{polymer})(k_1 \exp(\frac{-E_1}{(R_{GC}T)})(1 - AR)) \tag{14}$$

The rate of polymerisation is given as

$$\frac{dm_{Pj}}{dt} = -m_{Pj}(k_1 \exp(\frac{-E_1}{(R_{GC}T)})(1-AR)) \quad +m_{Lj}((k_2 \exp(\frac{-E_2}{(R_{GC}T)})+k_3 \exp(\frac{-E_3}{(R_{GC}T)}))AR) \tag{15}$$

Only the non-aromatic molecules exit the liquid phase through thermal cracking and this leaves only the aromatic fraction of the fuel in the liquid phase. This leads to an increase in the aromaticity of the liquid phase which is given as

$$\frac{dAR}{dt} = k_1 \exp(\frac{-E_1}{(R_{GC}T)})(1 - AR)AR \tag{16}$$

The coefficients used in equations 14, 15 and 16 are presented in table 2. As stated earlier the pyrolysis model used here is based on the work of Baert. Garaniya used the same model but with modified parameters and further adjustments have been made to the parameters in the present work.

Table 2: Coefficients used for the pyrolysis model in this model as well as the works of Baert[14] and Garaniya[3]

Coefficients	Baert's model	Garaniyas modified model	Present model
k_1 (1/s)	2E7	8E7	16E10
k_2 (1/s)	8E6	5E7	5E7
k_3 (1/s)	1E13	1E13	1E13
E_1 (kJ/mol)	$125E3$	85E3	85E3
E_2 (kJ/mol)	100E3	90E3	90E3
E_3 (kJ/mol)	270E3	270E3	270E3

3.1.3 Polymer oxidation

When most of the volatile compounds present in the beginning have left the droplet through evaporation and pyrolysis, the carbonaceous residue, that was created through polymerisation, will start to oxidise. This is known as the polymer burnout phase. In the present model the burnout of polymer is modelled in a process analogous to the char burnout model in Star-CD. The polymer burnout phase in the present model is allowed to begin once the aromaticity of the droplet has reached 0.9 and 95 % droplet has been converted into polymer.
Similarly to the combustion model, the burnout of polymer is controlled by a combined rate coefficient. The combined rate is a combination of the diffusion rate and the chemical rate and the burnout of polymer can be controlled by either one of these. The diffusion rate coefficient can be given as

$$K_d = 5.06 \cdot 10^{-12} \frac{T_{ref}^{0.75}}{d} \tag{17}$$

where T_ref is the reference temperature and d is the droplets diameter. The chemical rate coefficient can be given as

$$K_c = A_{poly} \exp(\frac{-E_{poly}}{R_{GC}T}) \tag{18}$$

where A_{poly} is the pre exponential factor for polymer E_{poly} is the activation energy for polymer. The value used for A_{poly} in the present model is 1.3 $kgm^{-2}s^{-1}(Nm^{-2})^{-n}$ and the value for E_{poly} is $9.27 \cdot 10^7$ J/kmol. The combined rate coefficient is then calculated as

$$q = (\frac{K_c K_d}{K_c + K_d})P_g \tag{19}$$

where P_g is the partial pressure of oxygen in the surrounding medium. The rate of polymer burnout is dependent on the rate coefficient as well as the surface area of the droplet and can be calculated as

$$\frac{dPoly}{dt} = q\pi d^2 \tag{20}$$

3.1.4 Droplet properties

As the lighter species evaporate from the droplet and its composition thus changes, some of the droplets properties will also change. The enthalpy of evaporation for each of the components, h_{fgj},is given as;

$$h_{fgj} = \frac{TY_j \Phi_{Hj}}{\theta_{Lj}} \tag{21}$$

where

$$TY_j = a_j + (b_j/B_j) * (\theta_{jR} y_{FjR}(1 + B_j) - \theta_\infty y_{fj\infty}) \tag{22}$$

and

$$\Phi_{Hj} = (T_{CRj} - T)^{0.38}/c_j \tag{23}$$

The constants a_j, b_j and c_j in equations 22 and 23 are constants that differ for each of the components. The critical temperature of the component T_{CRj} is given as;

$$T_{CRj} = a_{crj} + (b_{crj}\theta_{jR}) \tag{24}$$

where a_{crj} and b_{crj} are again component specific constants. To get the heat of evaporation for the Residue fraction that evaporates only through pyrolysis the heat of decomposition $h_d = 4.0e7 \cdot EXP(-2.7 \cdot T_C/T_D)$ is added to the enthalpy of evaporation. Finally the specific heat of the liquid phase for each component, C_{pLj}, is calculated as

$$C_{pLj} = 1000(a_{cp} - (b_{cp}T_D) + (c_{cp}(T_D^2)) \tag{25}$$

where a_{cp}, b_{cp} and c_{cp} are component specific constants. Viscosity and the surface tension coefficient are kept constant at values of 0.0135 kg/ms and 0.04 N/m respectively.

3.1.5 Application to modelling Cenosphere emissions

The focus of this thesis is to model emissions of cenospheres. However, the model described above is not designed for the sole purpose of doing this and does not contain a single term that would describe emissions. It simply models all the masstransfer processes that take place for each droplet. The possibility to use this kind of a model to simulate cenosphere emissions is due to the fact that cenospheres are what is left of the fuel droplets once all the masstranfer processes have taken place. In the absence of sufficient oxygen or time for complete oxidation of the polymer through the polymer burnout phase, the polymer that is left will be emitted from the process as cenospheres. By looking at what is left of the droplets at the end of the simulation it is therefore possible to apply this model to simulating cenosphere emissions.

3.2 Important submodels for spray combustion

As the present model does not simply create a passive soot scalar that does not influence the other sub-models in the simulation, this mass-transfer sub-model cannot simply be added to a functioning model without consideration for its effects on the simulation as a whole. Many sub-models that are important in spray combustion need to be considered and optimized in order for the whole combustion model to work properly. In the following subsections some of the most important sub-models influencing the performance of the simulations are presented and the choice of models and parameters are motivated.

3.2.1 Computational Grid

The computational grid used for the simulations in this study was developed by Kaario[32]. It is a sectional model representing a section of the cylinder in the Wärtsilä W20 engine. The mesh used in the model consists of 185665 cells and it is a moving mesh configuration where layers of cells deform and are collapsed and re-activated to model the movement of the piston. Figure 3 shows the computational grid at two different time steps.

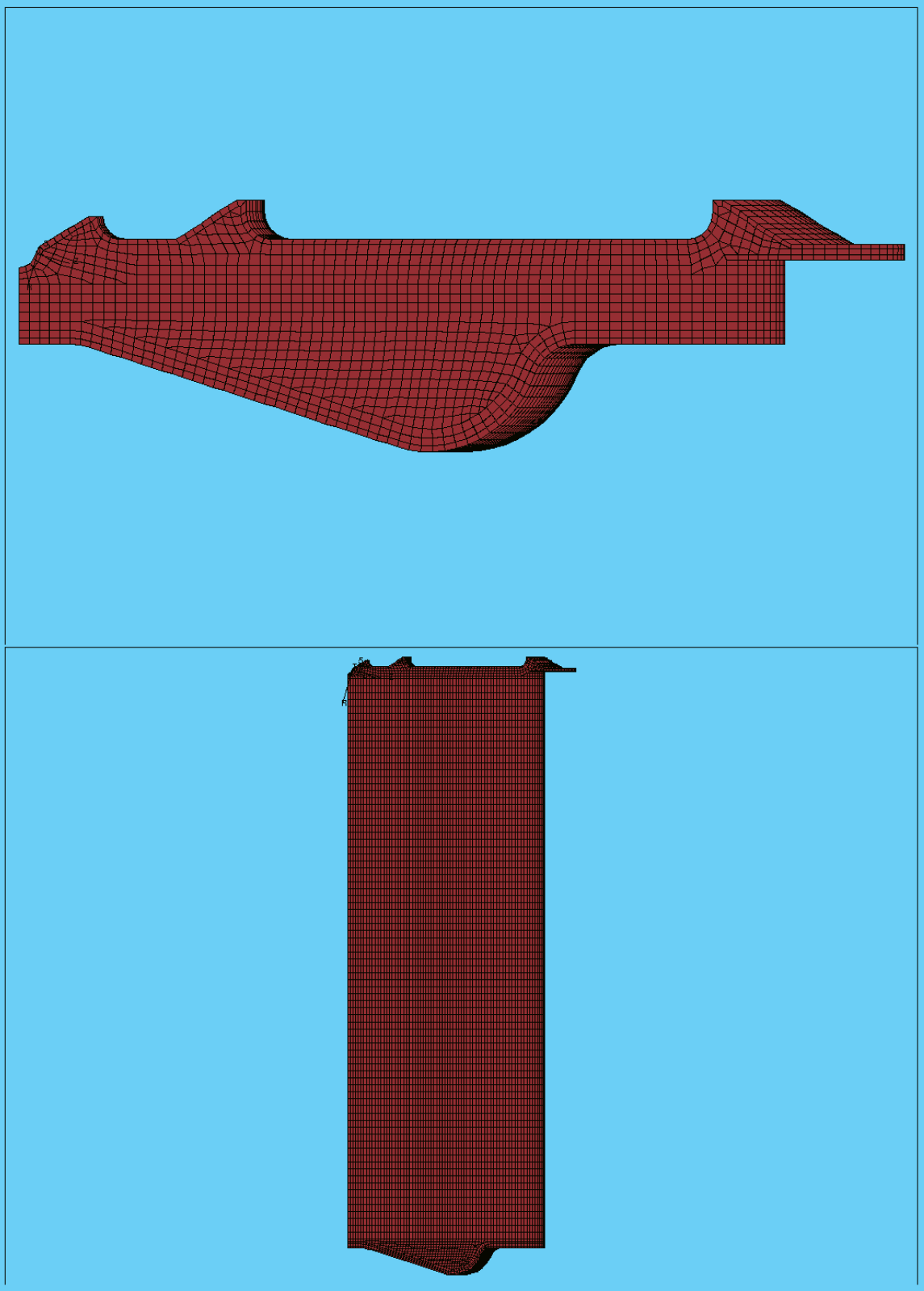

Figure 3: The computational grid used in the simulations, shown at both initial piston position and at crank angle 360°

3.2.2 Combustion and ignition

The Laminar and Turbulent Characteristic Time combustion model(LaTCT), introduced by Abraham et al. [33] was used to model combustion along with the shell auto-ignition model, a combination which was first introduced to diesel engine modeling by Kong et al.[34]. The standard shell auto-ignition model parameters in Star-CD were used apart from the time-range when the model is active. The start time for ignition was set to match experimental data for each load case and the end time was set to a point late in the cycle to allow model conditions to determine when ignition occurs. The LaTCT combustion model was implemented into Star-CD using a user-subroutine developed by Kaario[32]. In the LaTCT combustion model the combustion rate is determined by a combination of chemical and turbulent time-scales. The characteristic time that combines the two aforementioned time-scales is given as

$$\tau_C = \tau_{ch} + f_{delay}\tau_\epsilon \tag{26}$$

where τ_C is the characteristic time, τ_{ch} is chemical time-scale, f_{delay} is a delay function and $f\tau_\epsilon$ is the turbulent mixing time-scale. The delay function f_{delay} is given as

$$f_{delay} = (1 - e^{-p})/0.632. \tag{27}$$

The term p in the equation above is the ratio of products to the reactive species. The delay function f essentially decreases the influence of turbulent mixing before combustion has started and then allowing it to increase as combustion proceeds.[32] The reaction rate determined by the characteristic time-scale can be given as

$$\frac{dY_{fuel}}{dt} = \frac{W_l W_t}{W_t + fW_l} \tag{28}$$

where W_l is the chemically limited reaction rate and W_t is the reaction rate limited by turbulent mixing. W_l can be calculated as

$$W_l = A_{ch}[Fuel]^{0.25}[O_2]^{1.5} exp(-E/RT) \tag{29}$$

where A_{ch} is the pre-exponential factor that should be set according to the case, E is the activation energy, T the temperature and R is the universal gas constant. The reaction rate determined by turbulent mixing is computed from

$$W_t = C_M \rho \frac{\epsilon}{k} min(m_{Fuel}, \frac{m_{O_2}}{r}) \tag{30}$$

where C_M is a model constant,ρ is the gas density, and r is stoichiometric oxygen to fuel ratio. The constants used for the LaTCT model in the present study are presented in table 3. For comparisont also the constants used by Kaario et al. are presented.[32]

3.2.3 Turbulence

A proper choice of turbulence model is very important for the performance of a CFD-model[3]. After testing several different turbulence models the best performance

Table 3: Model constants used in present study and in study by Kaario et al.

	C_m	A_{ch}	E(kJ/mol)
Kaario et al.[32]	3	4000	77.3
Present study	6	8000	77.3

was found with the RNG k-ϵ model. However it turned out to be necessary to modify the standard model settings in Star-CD in order to get the best performance. The standard RNG k-ϵ model predicted low cylinder pressures compared to the available experimental data. This was in accordance with the findings of Kaario [32] and the modification of the model parameters suggested in his dissertation, The Influence of Certain Submodels on Diesel Engine Modeling Results, were adopted. The constants used for the turbulence modeling are presented in Table 4.

Table 4: Values for RNG k-ϵ turbulence model constants

	C_μ	C_1	C_2	C_3	σ_k	σ_ϵ
Std RNG k-ϵ	0.085	1.42	1.68	-0.387	0.719	0.719
Modified RNG k-ϵ	0.085	1.42	1.68	-1.0	0.719	0.719

3.2.4 Atomization and droplet breakup

The droplet breakup regime determines the sizes and numbers of droplets produced in the simulation. As every droplet results in a coke particle once all lighter components have evaporated, the atomization and breakup models therefore have a large impact on the particle emissions predicted by the present model. As no detailed experimental data on PM emissions, such as particle size distributions, from the studied case was available, it is difficult to determine the best droplet breakup model to use. The effect of the droplet breakup regime on the PM emissions predicted by the present model and the overall performance of the model is studied by testing two different droplet breakup models in Star-CD. Both models were tested with the standard settings and two sets of modified parameters partly to attempt to achieve optimum performance of the model and partly in order to study the effects of model settings on the results.
Star-CD currently has the following 4 different breakup models available:[35]

- Reitz and Diwakar model
- Pilch and Erdman model
- Hsiang and Faeth model
- KHRT model

The droplet breakup models were often developed to be used with lighter distillate fuels, and it is not therefore clear that optimum performance can be expected from all these models when using HFO as fuel.[3] The viscosity of HFO is often much higher than that of distillate fuels and experiments have shown that viscosity can affect the droplet sizes in a diesel spray.[36] The Weber number is used to determine the breakup regime a droplet experiences. The Weber number is defined as

$$We = \frac{\rho_g u_{rel}^2 D_d}{2\sigma_d} \tag{31}$$

where ρ_g is the gas density, u_{rel} is the relative velocity of the droplet, D_d is the droplet diameter and σ_d is the surface tension coefficient. At low Weber number values the droplet stays stable and as the number increases the droplet goes through different breakup modes. Typically low viscosity droplets remain stable while We<12 while higher viscosity droplets can remain stable at higher weber numbers.[36] Ideally the breakup model used in HFO diesel combustion would then both take into account the high viscosity of the fuel and the high Weber numbers encountered in diesel spray combustion.[36] The Hsiang and Faeth model is not valid for high Weber number cases as it lacks a high Weber number breakup regime and is therefore not a good choice for the present case. [36] The Pilch and Erdman model does not consider the droplet viscosity when determining the stable droplet size and is therefore also not an optimal choice for HFO combustion modeling. [36]

The Reitz-Diwakar is the simplest model available for droplet breakup and atomization in Star-CD and in lack of more detailed information about the studied spray it is often the best default choice[3]. Additionally while this breakup model is quite simple it does feature a breakup regime for high Weber number conditions and could thus feasibly be applied for diesel combustion processes [36]. Therefore the Reitz-Diwakar model was chosen as an breakup model to be used in this study.

The secondary breakup of droplets is modeled by two droplet breakup regimes:

- Bag breakup
- Stripping breakup

Both regimes have their own criterion for instability and for the characteristic timescale of breakup.

The Bag breakup process is analogous to the Rayleigh-Taylor instability and is a process where non-uniform pressure around the droplet causes the droplet to deform and ultimately disintegrate as surface tension forces are overcome[3]. In this regime the instability is determined by a critical value of the weber number as follows[35];

$$We \geqslant C_{b1} \tag{32}$$

where C_{b1} is an empirical coefficient. The associated characteristic time for the droplet breakup is[35]

$$\tau_b = \frac{C_{b2}\rho_d^{1/2} D_d^{3/2}}{4\sigma_d^{1/2}} \tag{33}$$

where C_{b2} is a model constant that is roughly equal to π .
Stripping breakup is a process where liquid is stripped off from the droplet surface due to tangential forces[3]. The criterion for the onset of this breakup is[35]

$$\frac{We}{\sqrt{Re_d}} \geqslant C_{s1} \tag{34}$$

where C_{s1} is a model constant with the value 0.5 and Re_d is the Reynolds number for the droplet which is given as

$$Re_d = \frac{\rho_d u_{rel} D_d}{\mu} \tag{35}$$

where μ is the viscosity of the droplet. The characteristic time-scale for the stripping breakup process is calculated as[35]

$$\tau_b = \frac{C_{s2}}{2}\sqrt{\frac{\rho_d}{\rho_g}}\frac{D_d}{u_r el} \tag{36}$$

where C_{s2} is a model constant. For both breakup regimes the change in the diameter of unstable droplets is calculated as[35]

$$\frac{dD_d}{dt} = -\frac{D_d - D_{d,stable}}{\tau_b} \tag{37}$$

where $D_{d,stable}$ is the droplet size that satisfies the equality in equations 32 and 34. Garaniya proposed the Reitz-Diwakar breakup model to be used with this droplet evaporation subroutine, along with modified parameters that were set to match visual experimental results[3]. The Reitz-Diwakar model settings proposed by Garaniya were tested as an alternative for the standard model settings in Star-CD. Additionally another modified version of the Reitz-Diwakar model was tested, this time with $C_{s2} = 15$, in order to show the effect of this parameter. The three sets constants for the Reitz-Diwakar breakup model that were tested are presented in table 5.

Table 5: Both the standard and modified constants used for the Reitz-Diwakar breakup model

	C_{b1}	C_{b2}	C_{s1}	C_{s2}
Modified R-D[3](Reitz-Diwakar 1)	8.4	0.5	4	26
std. R-D(Reitz-Diwakar 2)	6	0.5	π	20
Modified R-D 2(Reitz -Diwakar 3)	6	0.5	π	15

The Reitz-Diwakar model is not heavily affected by the viscosity of the fuel[36] and therefore it would be interesting to study the importance of the viscosity of the fuel by also testing a model that takes it into account. The KHRT breakup

model is affected by droplet viscosity and therefore tests using both the standard settings in Star-CD and a set of alternative parameter values are included in this study. The KHRT model is a hybrid model combining models for Kelvin-Helmholtz (KH) instabilities and Rayleigh-Taylor (RT) instabilities. KH instability is due to aerodynamic forces acting on the droplet surface creating an unstable surface wave and causing liquid to be shed from the surface of the droplet. RT instability is caused by the deceleration of the droplet which causes the droplet to deform and ultimately break into smaller droplets.[35] In the KHRT model these two phenomena compete with each other and the one that predicts the fastest breakup will trigger a breakup event. In the implementation found in Star-CD an KH breakup event will shed mass from the parent parcel and create a new parcel with smaller droplets. The shedding of the child droplets is due to the development of an unstable surface wave and the parent droplet has an diameter larger than the wavelength $\Lambda_{KH}$of the wave. The size of the stable child droplets is calculated as

$$D_s = 2B_0\Lambda_{KH} \tag{38}$$

where B_0 is a model constant. The change in size of the parent droplet is calculated in a similar fashion to the Reitz-Diwakar model as

$$\frac{D_d}{dt} = \frac{D - D_s}{\tau_{KH}} \tag{39}$$

where τ_{KH} is the characteristic time for the KH breakup and is given as

$$\tau_{KH} = \frac{3.726B_1 D/2}{\Lambda_{KH}\Omega_{KH}} \tag{40}$$

where B_1 is a model constant and Ω_{KH} the growth rate of the fastest growing wave. The criterion for a RT breakup to occur is that that a time longer than the RT breakup time-scale τ_{RT} has passed since the last RT breakup and that the droplet diameter is larger than the wavelength Λ_{RT} of the fastest growing Rayleigh-Taylor wave scaled by a constant C_3 so that[35]

$$D_d > C_3\Lambda_{RT}. \tag{41}$$

The value of Λ_{RT} is obtained by finding the value of the corresponding wave number $k_{RT} = 2\pi/\Lambda RT$ that maximizes the growth rate of the wave calculated as

$$\omega(k) = -k^2(\frac{\mu_l + \mu_g}{\rho_l + \rho_g}) + \sqrt{k\frac{\rho_l - \rho_g}{\rho_l + \rho_g}a + \frac{k^3\sigma}{\rho_l\rho_g} + k^4(\frac{\mu_l + \mu_g}{\rho_l + \rho_g})^2}. \tag{42}$$

The time-scale for RT breakup is then given as

$$\tau_{RT} = \frac{C_\tau}{\omega(k_{RT})} \tag{43}$$

where C_3 is a model constant that is commonly set equal to 1[35]. As can be seen equation 42 contains a term with the viscosity of the liquid μ_l and thus allows the

viscosity of the droplet to influence the breakup due to RT instability. This makes the KHRT model an interesting alternative in HFO simulations as HFO has such a high viscosity[36]. Two sets of parameters for the KHRT model were tested for this study, the standard settings in Star-CD and a set of alternative settings that where the settings were modified in order to get the best fit to the experimental data available. The starting point for the modified settings for the KHRT model were the settings found to work best by Bong[36] but the a value of 0.4 was used for the constant C_3 instead of the value of 1 suggested by Bong. A third version of the KHRT model was also used with the values of 6 and 0.1 for parameters B_0 and C_3 respectively. This was done to show the effects of changing the value of the C_3 parameter alone. The constants used for the KHRT model in this study are summarized in table 6

Table 6: The constants used for the KHRT breakup model

	C_3	C_τ	B_1	B_0
Std. KHRT(KHRT 1)	0.1	1	0.61	40
Mod. KHRT (KHRT 2)	0.4	1	0.61	6
Mod. KHRT (KHRT 3)	0.1	1	0.61	6

3.2.5 Gas phase soot model

In the present study the standard soot model in Star-CD was used with the standard settings. The 4.24 version of Star-CD does offer four alternative soot models but only the one equation laminar flamelet model developed by Mauss et al. was available for the combustion model that was used. This is a simple model that only gives the predicted mass of soot and its spatial distribution in the cylinder as output. It is not possible to get size distributions and the number of particles emitted from this particular model.[35]

3.2.6 Droplet collision and coalescence

The droplet evaporation subroutine that is the basis of the present model is not currently compatible with droplet coalescence and thus the collision model in Star-CD was turned off[3]. All other sub-models were tuned to give the best performance without the collision model.

3.2.7 Solution procedure

The PISO solution algorithm with coupled flow Lagrangian multiphase calculations is employed in this study. However as pointed out by Garaniya the droplet mass transfer and droplet properties subroutines used in this study are not compatible with the standard solution procedure for coupled flow[3]. As it was not possible to

correct this issue within the scope of this work, the "Predictor only" option was used in the simulations. This provides a faster but somewhat less accurate solution. It is possible that this could have led to some of the otherwise surprising convergence issues that were faced during the simulations.

3.2.8 Parameters for present model

The implementation of the present model into Star-CD includes the creation of 4 fuel components for the droplet. Also the initial amount of each of these component is to be specified. The initial concentrations of each component are specified in table 7. As can be seen the share of cutter stock was increased from 0.3 to 0.5 while keeping the compositon of the cutter stock the same. The increase in the share of the lighter components are partly motivated by the fact that the pressure level results obtained with 0.7 residue share were very low compared to experimental data for the case. Also these parameters should be set to match the fuel that is to be modelled, and based on the information available about the fuel used in the experiments, it is slightly different from the fuel characterized in Garaniyas work. The share of the ratio of cutter stock to residue for the fuel used in the experiments was unknown, but an elemental analysis was available. The HFO sample studied by Garaniya had a sulphur content of 4.5% [3]while the fuel used for the experiments for the studied case had a sulphur content of just 0.5%. Sulphur content can correlate with the content of asphaltenes in the fuel[18] and therefore it was concluded that reducing the amount of heavy residue could give a better approximation of the fuel in this case.

Table 7: The initial fractions of components used in the present model and the model suggested by Garaniya[3]

Component	Present model	Garaniya's model
n-Paraffins	0.25	0.15
Aromatics	0.083	0.05
Naphtenes	0.167	0.1
Residue	0.5	0.7

4 Results

In the previous chapters the implementation of the present model into the CFD code Star-CD 4.24 was described. In this chapter the simulation results will be presented and analysed. The results will be compared to available experimental data, both found in literature and available data from Wärtsilä for the particular case studied here, and the performance of the model will be evaluated. The choice of submodels and parameters will also be motivated and the effects of some of these settings will be studied.

4.1 Experimental results in literature

Finding suitable experimental results from the literature to evaluate the performance of the present model is quite challenging. The difficulty lies partly in the variation in the results due to differing measurement techniques and partly in the way particle emissions are formed in HFO combustion. Mass flow numbers alone tell only little about the performance of this model as a large amount of the total particle mass can stem from impurities in the fuel, such as ash and sulphur, and the present model is not designed to catch the formation of these. Additionally the present model actually contains two modes for particle formation, both a liquid and gas phase soot model. Therefore more detailed studies about the nature of the PM emitted from HFO combustion are needed in order to distinguish between the different kinds of particle emissions. Particle size distributions are of interest as well as studies on chemical characterizations of particles of different sizes.

Some studies fulfilling these needs were found in the literature. Moldanová et al. [37] studied the characteristics of PM emitted from a large ship diesel engine using residual oil. They found that the particle size distribution was bimodal with an additional peak in particle mass concentration at around 10μm in addition to the fine particle mode typically found in emissions from burning lighter fuel[37]. The findings of Moldanová et al. are in accordance with the findings of Lyyränen et al. who also found a peak in particle size distributions in the coarse mode around a particle diameter of about 10 μm in two separate studies[11], [38]. A study by Fridell et al.[39] also reported a bimodal size distribution with a second coarse mode peak at around 10 μm. Both Fridell and Lyyränen attributed the coarse mode peak partly to re-entrained particles from the combustion system surfaces that have grown through the addition of primary particles[39], [11]. The random nature of inception of re-entrained particles would partly explain the absence of the mode in some measurements[39]. However the mode is also likely partly due to char particles from incomplete combustion of fuel droplets.[11]
The larger particles found in the above mentioned studies are generally not reported in studies where particles were studied in ship plumes with for instance aerosol counters. This is likely due to the fact that while larger particles influence the mass flow of PM significantly, they are few in number compared to the small particles that are abundant in emissions from HFO combustion.[39]

The particle size distributions found in the studies mentioned earlier are presented in Figure 4. As can be seen most curves in figure 4 show a bimodal distribution

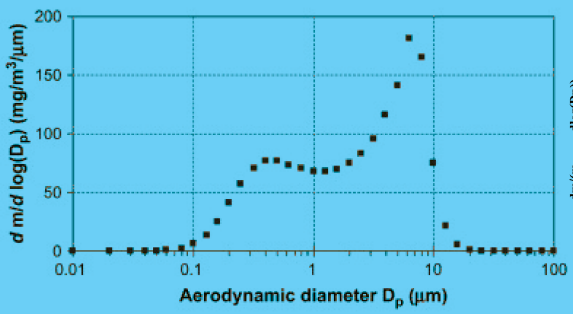

(a) Moldanová[37]

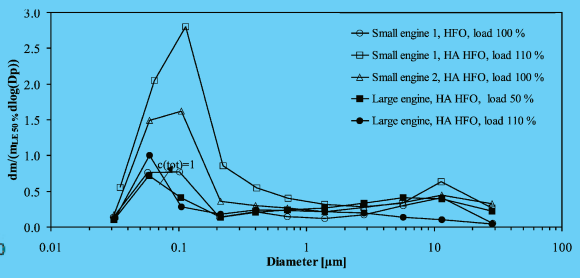

(b) Lyyränen[11]

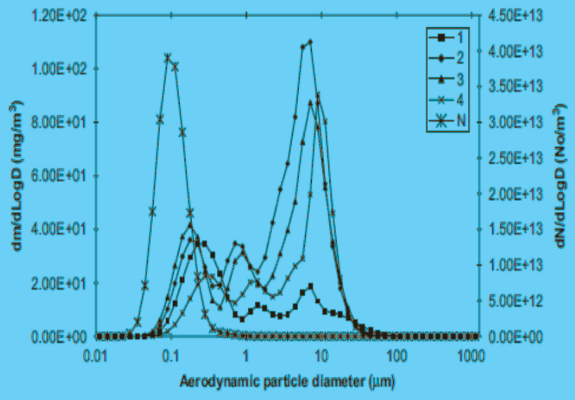

(c) Fridell[39]

Figure 4: Measured particle size distributions for large marine diesel engines running on HFO found in literature

with a peak in the coarse mode in addition to the fine particles commonly present in diesel combustion of lighter fuels. Also the presence of particles of all sizes between the two modes can be seen. The particle size distribution measured by Fridell et al.[39] is presented in figure 4c also contains a number-size distribution represented by the curve marked N. The number distribution shows that while the coarse mode particles have an influence on the mass of emissions the number of particles in the coarse mode is relatively small compared to the fine mode particles.

When analysing particles in HFO exhaust gases more closely Moldanová et al. they identified the following four distinct types of particles:[37]

- Soot particles
- Mineral/ash particles
- Organic particles
- Char and Char-mineral particles

Soot particles were found to be small, with a mean size of about 50 nm, and roughly spherical in shape. They are assumed to be nucleated from the volatilized compounds in the fuel and are essentially the emissions modelled by traditional soot models. The soot particles can also form agglomerates of many individual soot particles that can range in size to a few microns.
Ash particles originate from the inorganic compounds present in the fuel. As the ash content of HFO is significantly higher than in distillate fuels, also the amount of ash particles is much higher. Ash particles originate from the volatilized inorganic compounds in the fuel and form spherical particles of about 40 nm in size through nucleation.[11]

The char particles are the group that is of most interest from the point of view of this work. They are assumed to be the residue of the pyrolysis of the heavier compounds in the fuel droplets and are thus the emission mode modelled by the present model. Moldanová et al. found them to be roughly spherical with sizes ranging from about 0.2μm to about 5μm.[37] Also Lyyränen et al. reported carbonaceous particles that originated from the residue of fuel droplets[11]. They suggested that they might make a significant contribution to the particles observed between the two main modes, found at 0.1μm and 10μm[11]. Figure 5 shows images of the particles observed by Lyyränen et al.[11]. The images clearly show the difference in structure between nucleation mode particles and agglomerations of these and the fuel droplet residue particles which are also known as cenospheres. Although cenospheres are much larger than the nucleated particles, the smaller particles can form agglomerates that are of a similar size as the cenospheres. This makes the differentiation of these different particle emissions difficult even when particle size distributions are known, as there will be some overlap in the particle sizes produced by these two distinct formation mechanisms.

Sarvi et al. studied the chemical composition of PM emitted from a large scale medium speed diesel engine and found that when using HFO the share of carbon in the PM is decreased as load increases. Their hypothesis was that this was due to better burnout of carbon due to better availability of oxygen at high loads[40]. Bartle et al. found that the size distribution of emitted cenospheres seem to depend on the size distribution of droplets in the fuel spray[41]. This supports the fact that each droplet forms an cenosphere. They also found that the asphaltene content of the fuel influenced both the sizes of the droplets and the resulting cenospheres due to its influence on the viscosity of the fuel[41]. Villasenor et al. studied the effects of asphaltenes on HFO droplet combustion and found that while coke formation is not only dependent on asphaltene content of the fuel, high asphaltene content increases the burnout time for created cenospheres[42].

Figure 5: Images of nucleation mode particles(a), agglomerated nucleation mode particles(b) and fuel droplet residue particle(c). Adapted from Lyyränen et. al[11]

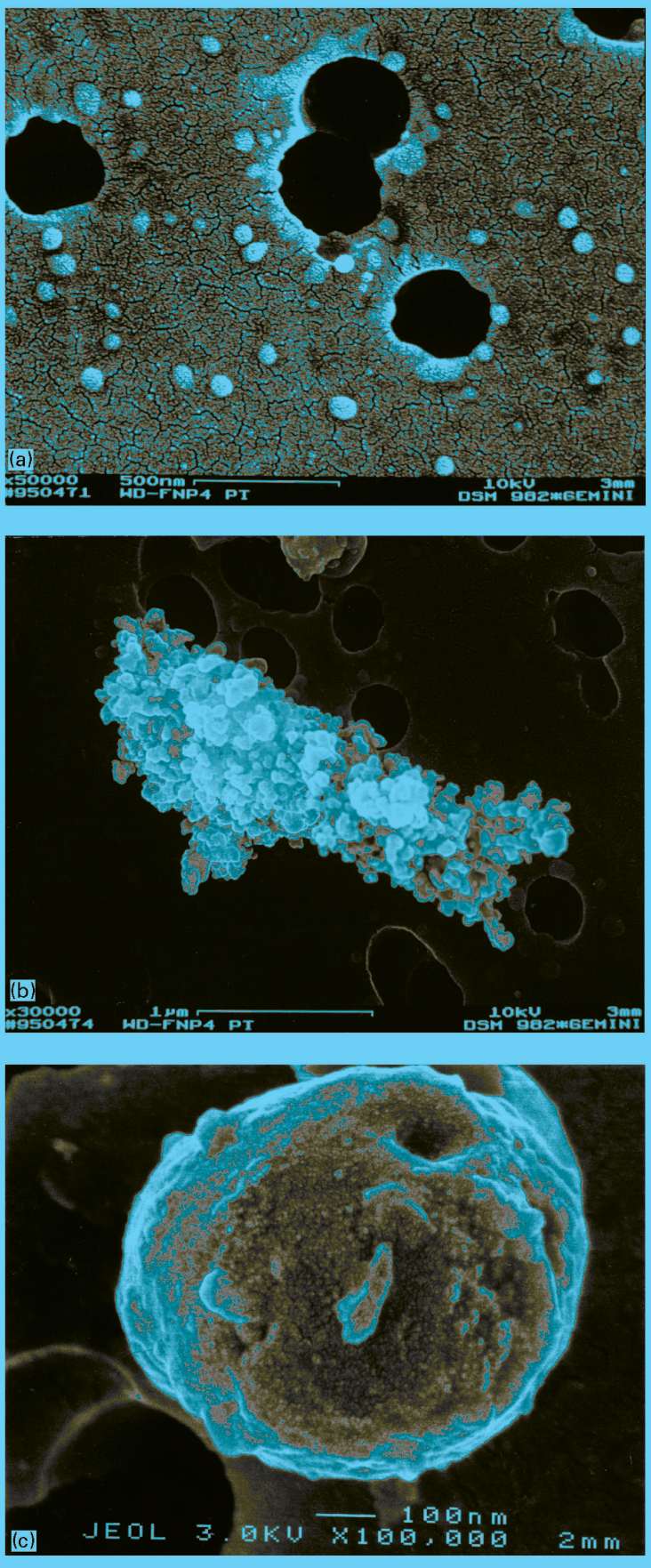

4.2 Simulation Results

In this section the results from the simulations performed for this study are presented. Where possible the results are compared to experimental results from literature in order to evaluate the performance of the present model and to motivate the choices of some submodels and model parameters. As this model gives the opportunity to change the properties of the fuel, the effects of some fuel properties on the results are also be examined.

4.2.1 Details about the case

As mentioned previously the simulation model used here is based on the Wärtsilä W20 engine. It is an engine with a cylinder bore of 200 mm and a stroke of 280 mm. The diameter of the injector nozzle holes in the case is 0.37 mm. The engine is run at a constant speed of 1000 RPM in all load cases but the duration of fuel injection is different for all three load cases. The times for beginning and end of injection in the simulation model are summarized in table 8. As can be seen injection starts

Table 8: Injection duration for each load case

Load	Beginning of injection (CA°)	End of injection (CA°)
100 %	354.611	388.703
50 %	354.708	375.266
10 %	355.012	363.905

around the same time but the end of injection is at very different times for the three load cases. As the effects of changes to some fuel properties are discussed later in this chapter a summary of the fuel properties used in the following model validation section is in order. The fuel properties used in the simulation model are as follows;

- Viscosity is constant at 0.0135 kg/ms
- Surface tension coefficient is constant at 0.04 N/m
- The density, specific heat and heat of vaporization of the fuel droplets are varied as the composition of the droplet changes
- The initial share of residue component in the fuel is 50 %. More detailed information about fuel composition can be found in table 7

There is experimental data available from test runs with the Wärtsilä W20 engine running on HFO. The available data is mainly average cylinder pressure measurements and this data is used for model validation in the next section.

4.2.2 Model validation

As mentioned in earlier sections the present model not only models emissions of particulate matter in a new way but also changes the way fuel properties and droplet evaporation is modelled. This means that in order to get decent performance from this model settings of a multitude of other submodels also need to be considered, in addition to choosing the proper settings for the evaporation and fuel properties models.
Due to the lack of detailed emissions data from the specific case studied it is difficult to establish the optimal model settings to be used for this model when modelling particulate emissions. Instead attempts have been made to choose model settings in order to model the combustion behaviour according to cylinder pressure as well as possible. This way most submodel settings can be chosen in order to establish a base-line case, to which the effect of altering key model settings and submodels can then be compared. The settings used for the these initial simulations are those described in the previous sections. The droplet atomization model chosen for the baseline case is the modified version of the Reitz-Diwakar model deskribed in Garaniyas work. This was used as reference as it was successfully used in Garaniyas original work with this model.

The average cylinder pressures predicted by the present model are presented in figure 6. The single component mode presented here uses similar sub-model settings as the present multi-component model but uses the standard mass-transfer routine in Star-CD. As can be seen in figure 6a The predicted pressure with the present model is slightly low for the 100 % load case, both with regards to peak pressure and pressure levels during the expansion stroke. The single component model gives a better prediction of pressures in the 100 % case. The low predicted pressures with the present model in the 100 % case are likely due to slower evaporation with this model. Attempts to increase the amounts of fuel vapour and consequently the pressure levels were made by changing the composition of the fuel and speeding up the production of pyrolysis gas by changing the pre-exponential factor for thermal cracking as presented in table 2. As the pressure after these changes, presented in figure 6, is still somewhat low these changes could be considered reasonable.
The pressure predictions for the 50 % load case and the 10 % load case follow the trend of the higher load case in the sense that the predicted pressure for the expansion stroke are a bit to low compared to the experimental data, as can be seen in figures 6b and 6c. The predictions of peak pressure are slightly different as the predicted peak pressure is actually slightly high for the 50 % load case and closer to experiment for the 10 % load case. The model does seem to give reasonable predictions for ignition delay for all the cases.

Although the present model does not perfectly reproduce the pressures found in the experimental data for the case, the performance was deemed to be reasonable. Further optimization of the model could probably result in even better results when it comes to cylinder pressure, but finding better settings to use proved difficult with the

data that was available. More detailed data about the fuel used in the experiments could have been helpful for determining the best fuel properties and composition to use, which would then have enabled the optimization work to focus on tuning other submodels for the best performance with these. As there was some uncertainty about the precise nature of the fuel used in the experiments the decision was made to keep the changes to Garaniyas original model settings modest. The performance of the model in the context of pressure predictions was still deemed to be good enough as it is in order to use it to study the emissions of cenospheres, which is the main focus of this study.

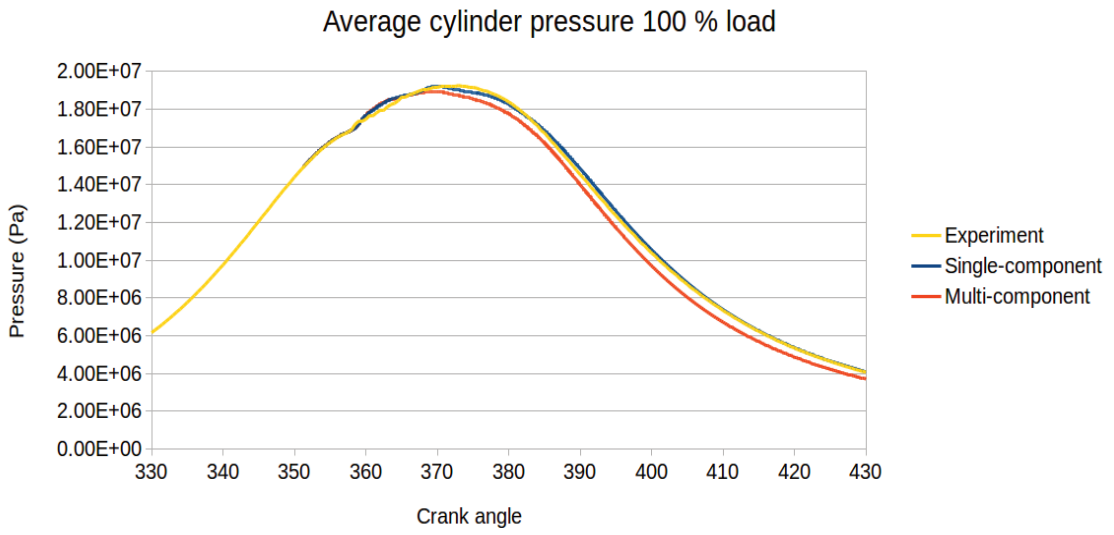

(a) Pressure at 100 % load

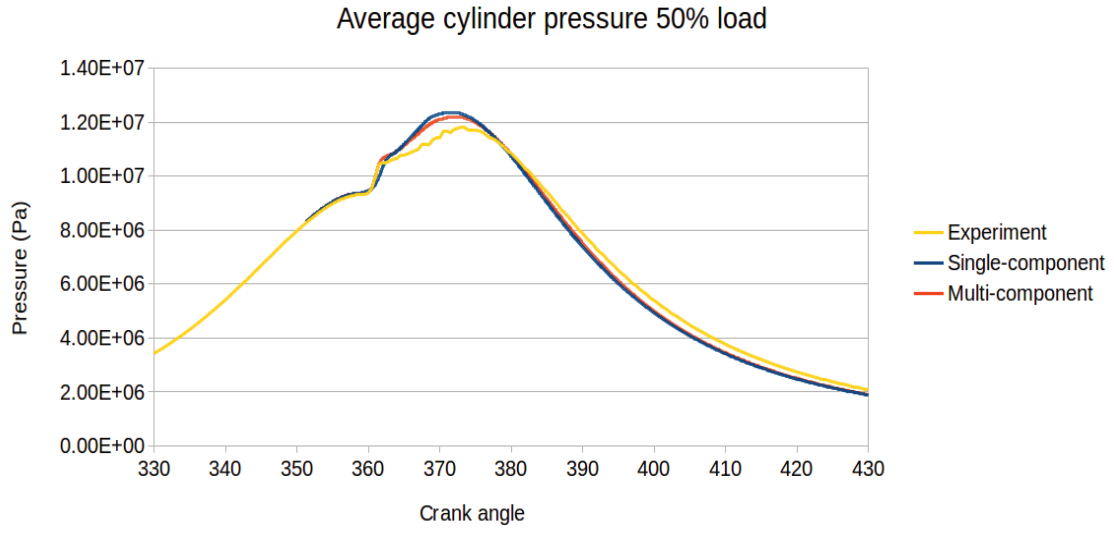

(b) Pressure at 50 % load

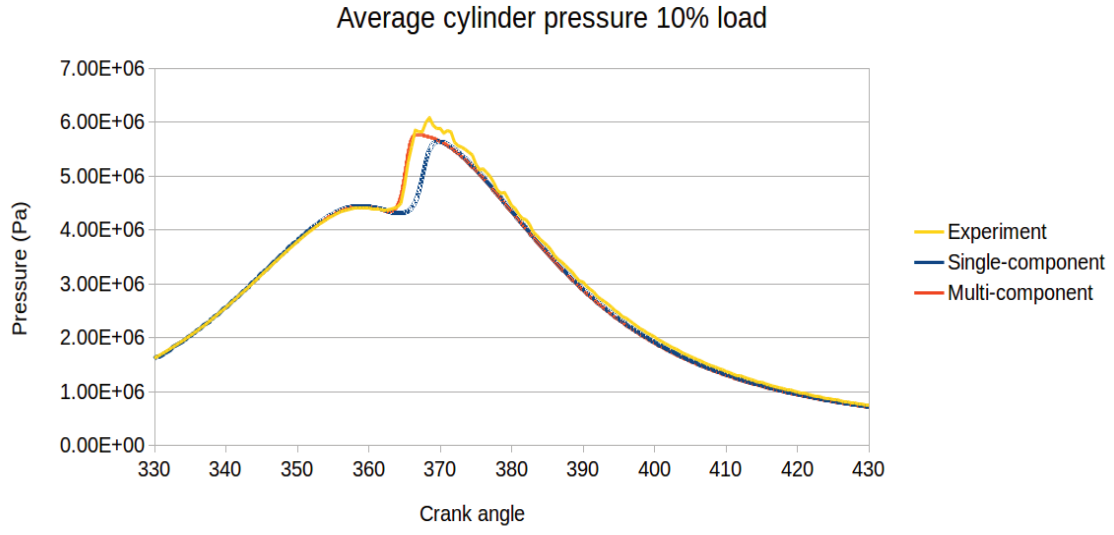

(c) Pressure at 10 % load

Figure 6: Average pressures at different loads with the present model, a single component model for comparison and according to experimental results for the case.

4.2.3 Results with standard model settings and effect of engine load on emissions

The predicted particle size distributions for cenosphere emissions are presented in figure 7. As can be seen it would seem that lower loads result in a larger number of smaller particles. Higher load results in larger particles having a peak in mass concentration at particle diameter of about 10 μm. The lack of smaller particles at higher loads means that number concentrations are decreased as load increases. As the load decreases the peak in both number and mass concentrations shifts toward smaller particles. It should however be noted that larger particles are also present in the lower load cases, just in significantly smaller numbers than the smaller particles.

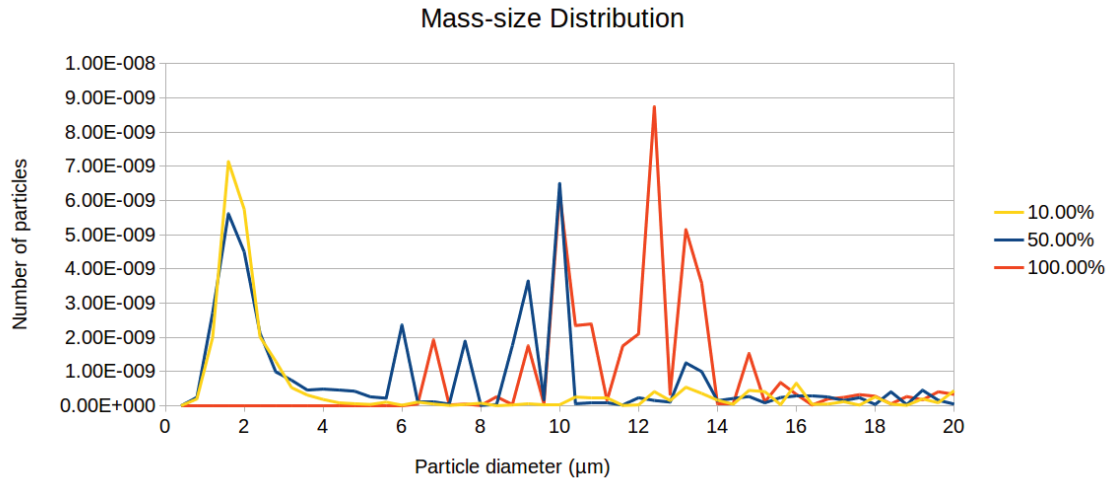

(a) Predicted mass-size distributions of cenospheres at different loads

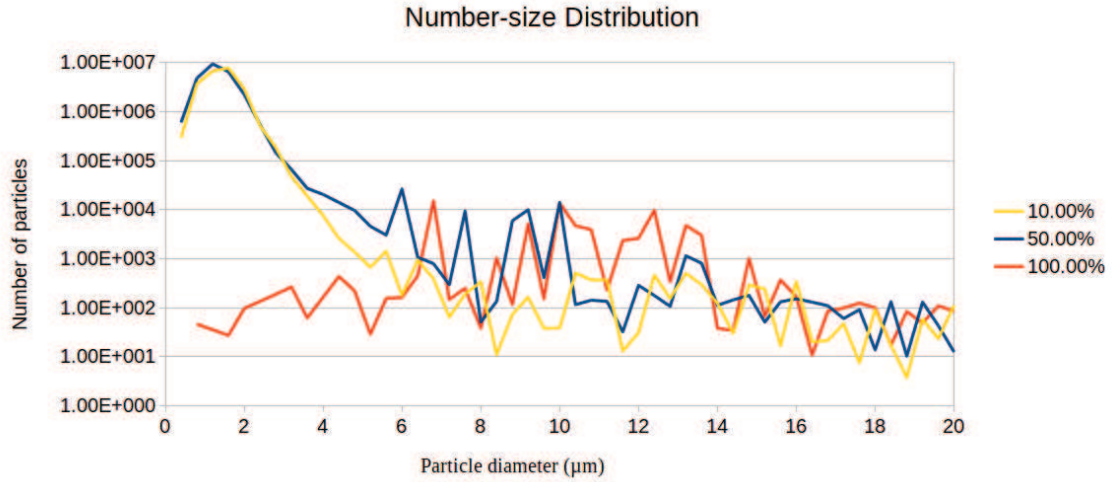

(b) Predicted number-size distributions of cenospheres at different loads(note the logarithmic scale on the y-axis)

Figure 7: Particle size distributions for predicted cenosphere emissions

The trend of smaller particles with decreasing load is interesting and it is worth studying the reasons behind this. One way to gain insight into the diameters of the emitted cenospheres is to study the evolution of the droplet diameters during the simulation. Figure 8 shows how the sauter mean diameter (SMD) of the droplets changes during the simulation. It can be observed that the evolution of the SMD follows a similar pattern on all three load cases. The diameter initially drops heavily after the start of injection. Then as the injection starts to slow down, the SMD suddenly increases again. After the end of injection the SMD falls once again only to peak again a little later and finally to descend slowly to a plateau. Conclusions that can be drawn from figure 8 are that the large particles found in the 100 % load case are created at the end of the injection and that the average particle size was still decreasing at the end of the simulation in the 100% load case. The slow decrease of the SMD toward the end of the simulation is likely due to the heterogeneous burnout of the cenospheres. The fact that this decrease stops earlier in the lower load cases could be because the low temperature and other conditions cause this reaction to cease earlier during the expansion stroke. As mentioned earlier, the SMD drops initially after the end of injection. This is likely due to droplet breakup, and that the SMD then starts increasing again would be due to the fact that the smallest droplets completely burn out and disappear, which only leaves the larger droplets in the simulation. The higher SMD in the 100 percent load case would then be caused by both large droplets created at the end of injection and better burnout of smaller droplets. The reasons for better burnout of cenospheres in the high load case are both higher temperatures and higher concentration of oxygen in the cylinder during the entire expansion stroke.

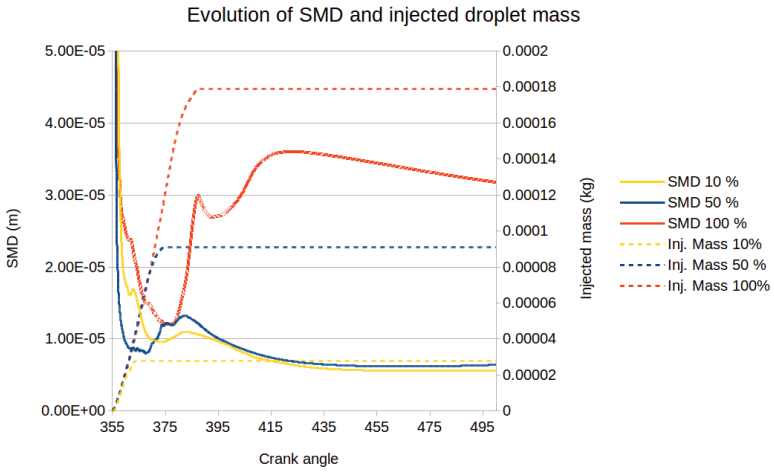

Figure 8: The evolution of the SMD of the droplets and the injected fuel mass during the simulation.

The presence of smaller droplets even in the high load case can be confirmed by studying the evolution of the droplet size distributions during the simulation. Figure

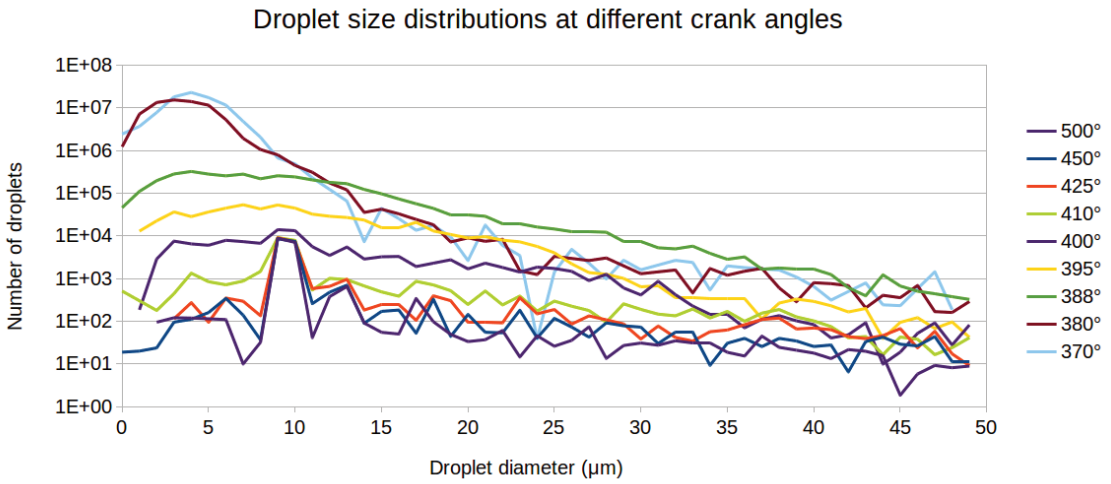

Figure 9: The droplet size distributions at different crank angles for 100 % load case

9 shows how the droplet size distributions change over time in the high load case. It can be seen that the size distributions remain similar, with a large amount of smaller droplets, under ongoing injection from 370° to 380°. The amount of smaller droplets then decrease and there is an increase in larger droplets in the range of about 15 μm to 35μm as the end of injection is reached at around crank angle 388°. At this point the distribution is quite flat compared to its final form at crank angle 500°, but as the simulation progresses toward its end the droplets smaller than 10 μm are consumed and at a higher rate. Larger droplets break into smaller droplets and thus a peak consentration at about 10μm is created. As no droplet coalescence model is active the reason for the lack of smaller droplets evaporation, and as the conditions in the high load case are more favourable for evaporation, it makes sense that more of the smallest droplets are consumed than in the lower load cases.

While the total emitted mass in absolute terms from the 100 % case is the highest that does not actually mean much as the higher load naturally means both higher output and higher amount of injected fuel. It is therefore of interest to study the amount of emissions in relation to the injected fuel mass in order to evaluate how emissions at different loads relate to each other. Figure 10 shows the remaining mass of the droplets at the end of the simulation. By this time all lighter components will have evaporated so the leftover droplet mass equals cenosphere emissions. As can be seen the higher load cases give lower emissions relative to the amount of injected fuel. This trend mirrors the one predicted by the FSN values, although it should be noted that the correlation between FSN and cenosphere emissions is somewhat unclear. The small amount of unevaporated mass left in the single component case stems from a small number of large droplets left at the end of the simulation.

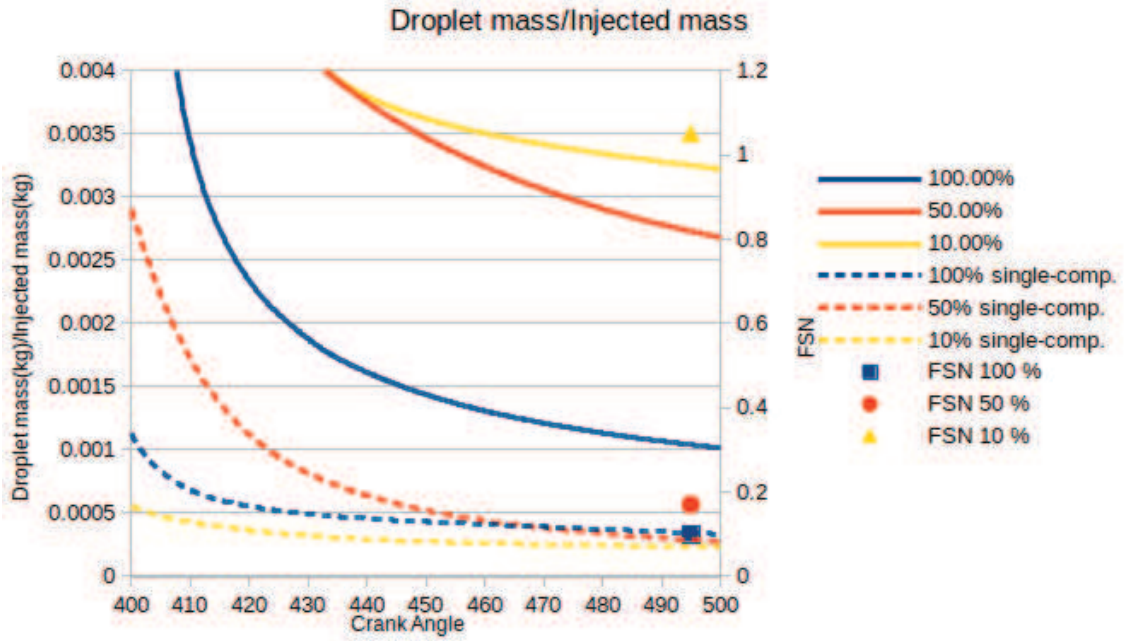

Figure 10: The mass of the remaining particles at the end of the simulation scaled by the mass of injected fuel. Results from single component model included for comparison as well as measured FSN values for the case

4.2.4 Effects of secondary droplet breakup model

Choosing an appropriate spray breakup model is crucial in any engine simulations. In this case however it is of particular importance as it will directly influence not only the combustion behaviour in the cylinder but also the size-distributions of the particles modelled by the present model. As discussed in previous sections two different spray breakup models were tested with three different sets of parameters for each breakup regime. The breakup models tested in this study were:

- The Reitz-Diwakar model
- The KHRT model

Changing the secondary breakup model will affect more than just the resulting particle size distributions from the simulations. It is therefore of interest to investigate the effect of these changes on the overall combustion behaviour in the model. This can be done by studying the average cylinder pressure predictions obtained with different breakup regimes. These are presented in figure 11. As can be seen the different settings of the breakup regimes affect the combustion but the differences in the cylinder pressures are not dramatic between the settings chosen for this study.

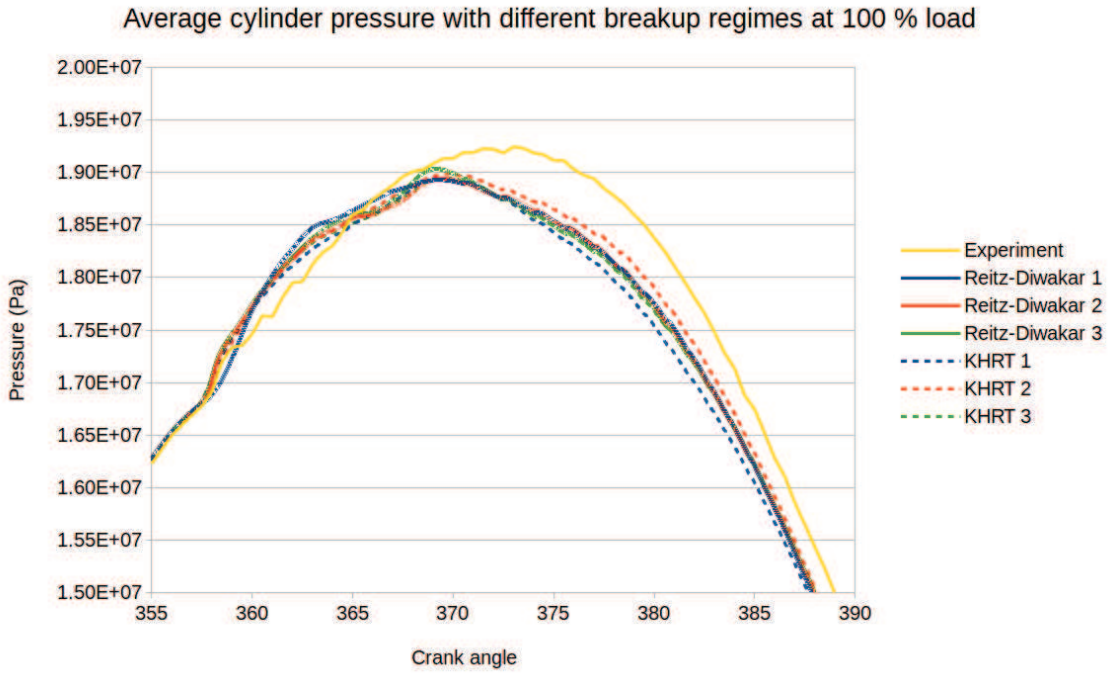

Figure 11: The average cylinder pressures with different breakup regimes at 100 % load

Without enough detailed data about the cenosphere emissions from the studied case it is not possible to decide which droplet breakup regime works best for this particular case. However trying out different breakup regimes does highlight the

differences in results produced by these models. Trying out different parameters on each model gives an understanding of how the parameters change the results and how important optimizing the secondary breakup model parameters is for getting accurate results.
The effects of the breakup models on emissions were tested in both the 100 % load case and the 10 % load case. The resulting particle size distributions from these simulations are presented in figures 12-15. The settings for the different breakup regimes can be found in the Implementation section in the tables 5 and 6 and the names in the legend of figures 12-15 correspond to those in the mentioned tables. While the range of droplet sizes presented in the following figures is limited to droplets smaller than 20μm it should be noted that larger particles are also present. Numerically they are relatively few but they do make a significant contribution to the total mass flow of PM. The decision to focus on the sub 20 μm is due to the fact that the peak concentrations do fall within this range as can be seen in figure 9. Also as far as emissions go the smaller particles are of most interest as they will travel further in the atmosphere, and are also far more abundant in numbers.
It can be observed form figures 12 and 13 that for the high load case the difference between the Reitz-Diwakar 1 regime, which uses the parameters proposed by Garaniya, and Reitz-Diwakar 2, that is standard version of the model, are quite small. The standard version produces slightly smaller droplets having most droplets in both mass and numbers in droplets with sizes of about 7-11 μm. Garaniyas version of the R-D breakup produced slightly larger droplets, as would be expected due to the higher values in model parameters, with peaks between 10 and 14 μm. In both these cases there was a relatively small amount of small particles present. Decreasing the coefficient C_{s2} in the third version of the R-D breakup model resulted in even smaller droplets with mass and number concentration peaks at both 5-7μm and below 2 μm. The standard KHRT model, here named KHRT 1, produced quite similar results to Reitz-Diwakar 1 & 2 with the addition of a smaller peak at below 2 μm. The two modified versions of the KHRT model produced very few droplets of diameters of below 20 μm compared to the other models. The high peak observed with the KHRT 3 version could be due to some kind of malfunction in the code as the data looked highly irregular. Overall the fast breakup in KHRT 2 & 3 did result in small droplets during the simulation, they were however quickly consumed through evaporation and therefore not present at the end. Both did however produce similar amounts of droplets larger than 20 μm as the other models.
For the 10 % case all the breakup models resulted in larger amounts of small particles. All the R-D versions produced similar results with the most small particles observed with the third version followed by versions 2 and 1 respectively. KHRT versions 1 & 2 also produced high amounts of particles smaller than 2μm but also had higher amounts of particles present in the 2-10μm range which is clearly reflected in the mass distribution presented in figure 14. Interestingly the KHRT 3 version produced results quite similar to the R-D models.
One conclusion that can be drawn from this comparison of breakup regimes is that all the models seem to preserve the trend of higher amounts of small particles with decreasing load. This would indicate that this is an effect of conditions in the cylinder

instead of only a function of different submodel settings. Also it can be concluded that a well functioning droplet breakup model is important for this kind of emissions modelling as there is significant differences between different models and settings, especially between KHRT 2 & 3 and the rest of the models in he 100 %*case* and KHRT 1 & 2 and the other models in the 10 % case.

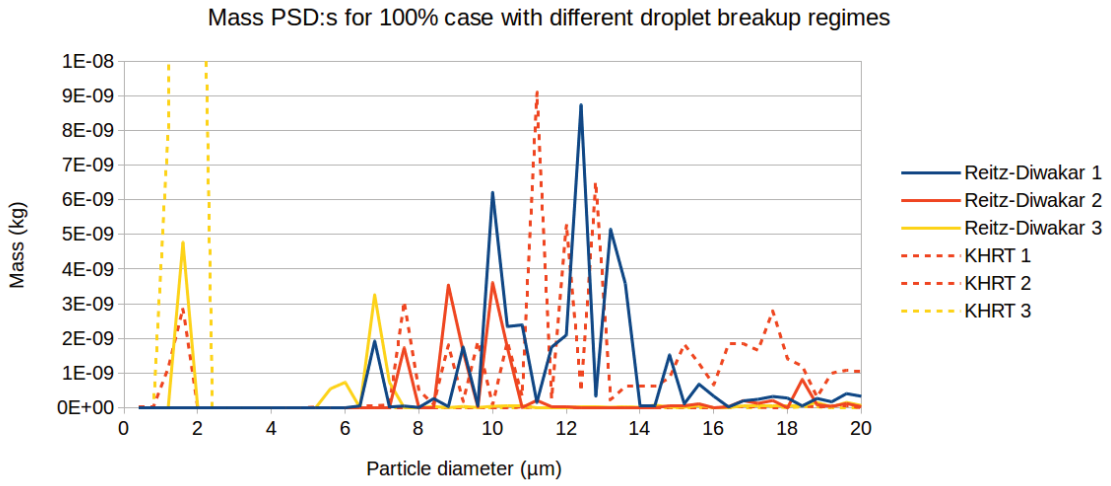

Figure 12: The particle mass size distributions produced by different breakup regimes at 100% load

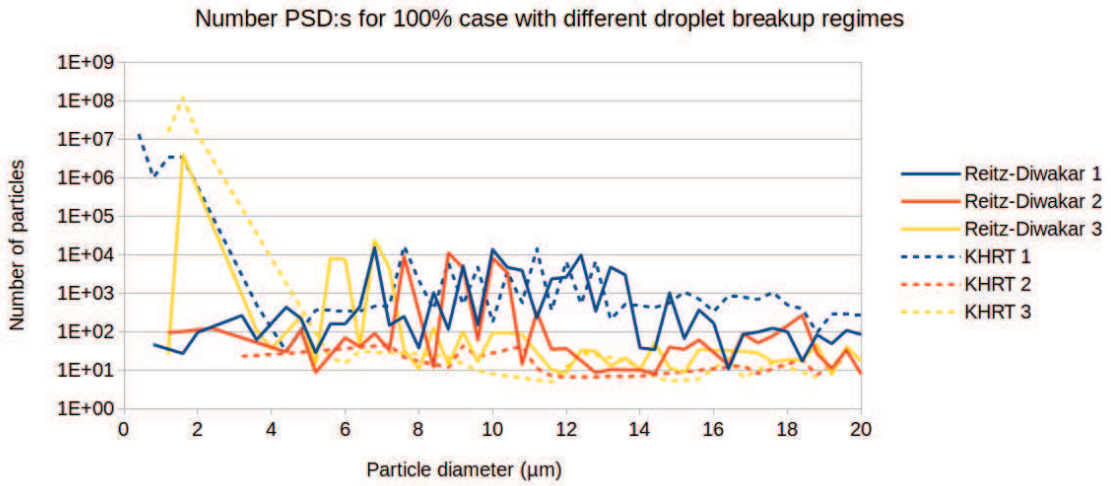

Figure 13: The particle number-size distributions produced by different breakup regimes at 100 % load

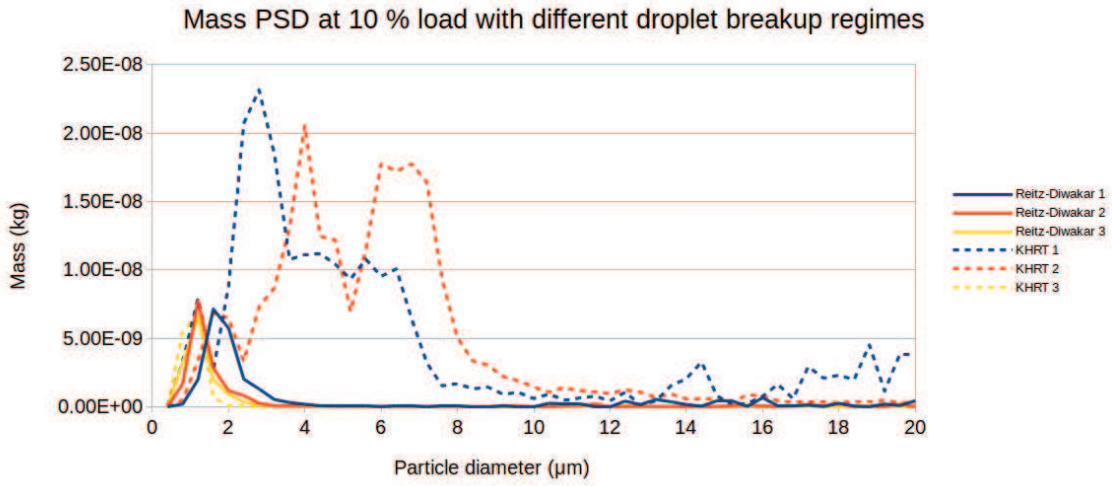

Figure 14: The particle mass-size distributions produced by different breakup regimes at 10 % load

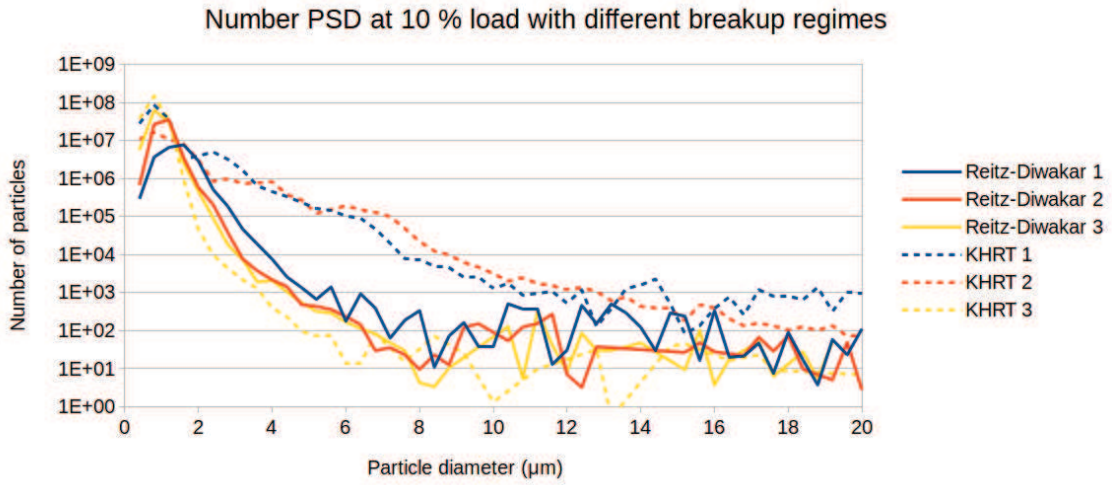

Figure 15: The particle number-size distributions produced by different breakup regimes at 10 % load

4.2.5 Effect of atomization on emissions

Changing the parameters on droplet breakup models presents the opportunity to artificially improve the atomization of the spray, leaving all other things the same. This way it is possible to study the effect of decreasing droplet sizes on emissions. The effect of breakup models on size distributions was already presented earlier and here the focus is on studying the effect on particle mass and number flows as atomization is improved.
To study the effect of smaller droplets the cases with Reitz-Diwakar breakup versions 1 and 3 are studied. To demonstrate that the third version of Reitz-Diwakar breakup, described in table 5, actually produces smaller droplets than the first version the SMD of the sprays with both the breakup models are presented in figure 16. As can be seen Reitz-Diwakar 3 clearly produces smaller droplets.

The effect of spray breakup on emissions can then be seen by comparing the remaining particle mass and numbers in each case. Table 9 shows how decreasing droplet sizes effects emissions of cenospheres. When it comes to mass of emitted particles, improving atomization clearly leads to lower emitted mass. This trend is the same for both load cases studied here. However improving atomization of the spray also leads to an increase in the number of particles emitted. It seems that while improved atomization does improve the burnout of particles, roughly halving the mass emissions of particles depending on the case, the burnout of smaller particles does not completely counteract the increase in the number of particles the improved atomization causes.

Table 9: The amount of droplets and droplet mass remaining at the end of simulation with different breakup regimes

Case	Total remaining droplet mass (kg)	Total remaining number of droplets
100 % R-D 1	1.82E-07	7.34E+04
100 % R-D 3	1.02E-07	4.03E+06
10 % R-D 1	8.98E-08	2.22E+07
10 % R-D 3	3.90E-08	1.03E+08

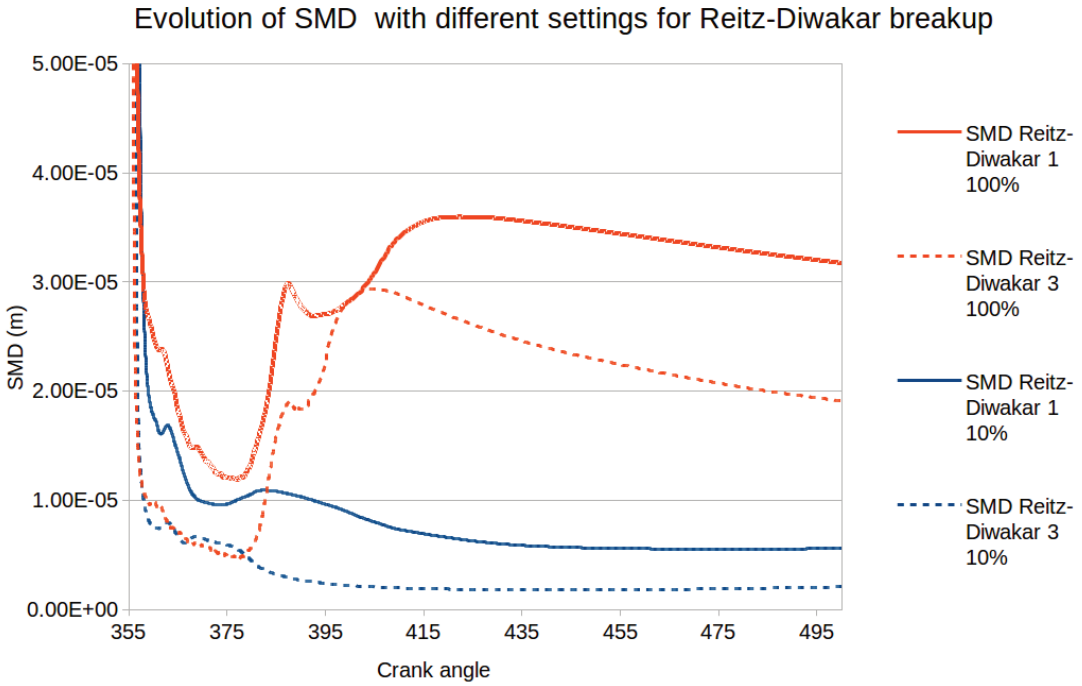

Figure 16: The SMD of droplets produced by vaiations of the Reitz-Diwakar breakup regime at 100 % and 10 % load

4.2.6 Effects of fuel properties

One of the interesting opportunities offered by the present model is the possibility to easily change fuel properties and composition. Therefore the effects of some key fuel properties will be examined here.

Viscosity As viscosity is one of the measurable properties that is used to describe different qualities of HFO and since different HFO:s can have quite different viscosities it is useful to study how sensitive these results are to changes in viscosity. Since the different secondary breakup regimes take the viscosity of the droplets into account in different ways, the effect of viscosity was tested with both the Reitz-Diwakar breakup model and the KHRT model.
The results of altering the viscosity of the droplets, presented in figures 17-20 show that with the Reitz-Diwakar model the effect of viscosity is relatively modest. However with the KHRT model, reducing the viscosity resulted in an significant increase in smaller droplets. This was expected as the two models treat viscosity differently, and point to the fact that if the effect of viscosity on cenosphere emissions is studied the KHRT breakup model should perhaps be preferred. In the present model viscosity is modelled as a constant, but if it was modelled as a function of for instance temperature this could have an effect on the particles predicted by the model, as viscosity does influence atomization of the spray.

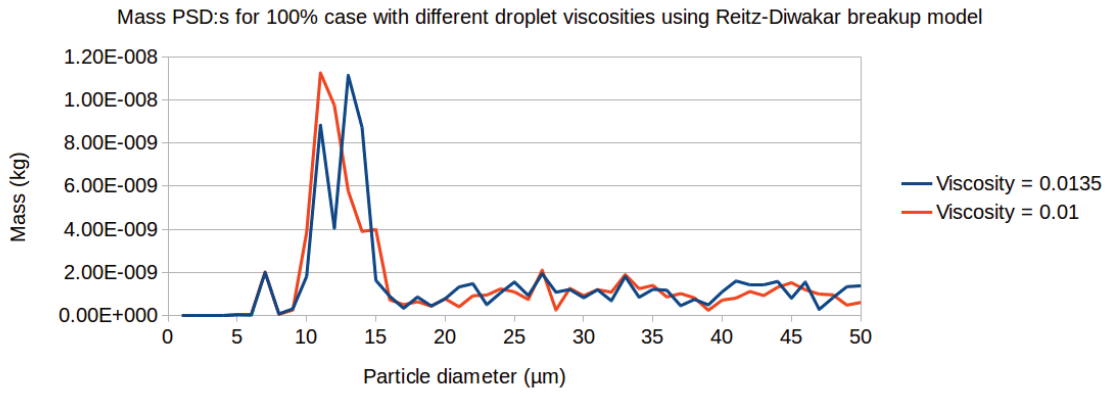

Figure 17: The particle mass-size distributions produced by different viscosities with Reitz-Diwakar breakup regime

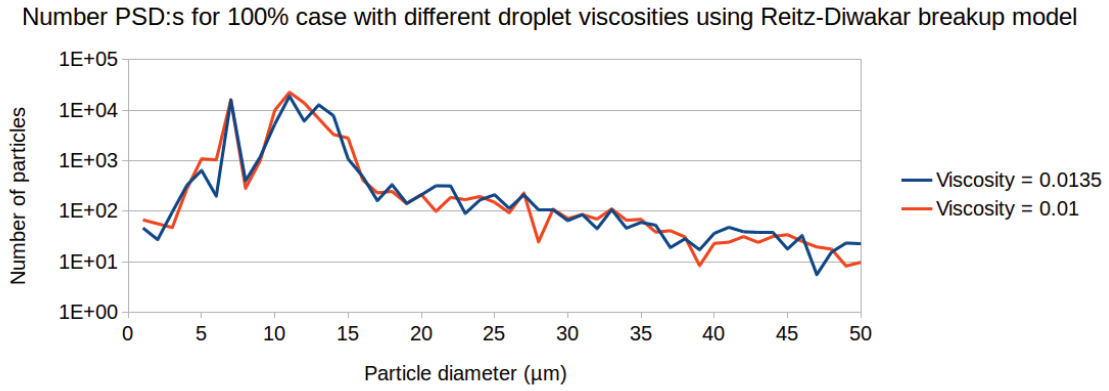

Figure 18: The particle number-size distributions produced by different viscosities with Reitz-Diwakar breakup regime

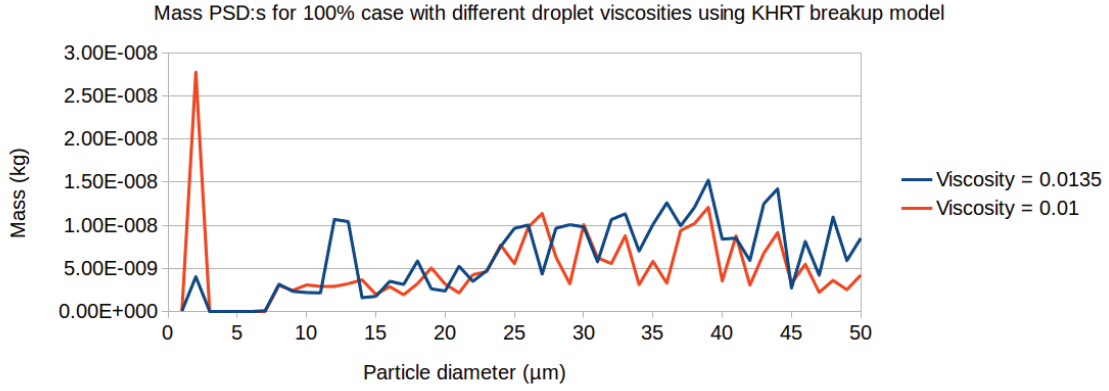

Figure 19: The particle mass-size distributions produced by different viscosities with KHRT breakup regime

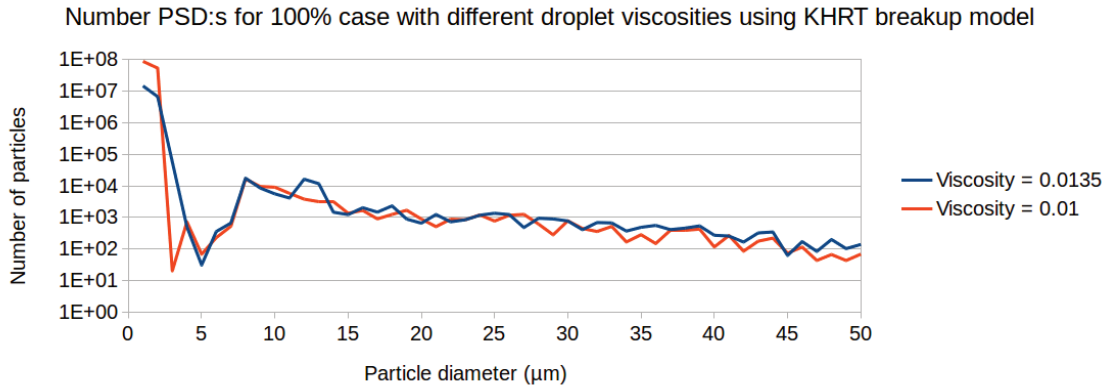

Figure 20: The particle number-size distributions produced by different viscosities with KHRT breakup regime

Fuel composition The present model also gives the opportunity of modifying the composition of the fuel. As many studies have indicated that heavy molecules such as asphaltenes influence the emissions of cenosphere it is of interest how this model reacts to changes in the amount of the residue component in the fuel. A higher amount of residue should lead to higher emissions. This holds true for the 100% case, presented in Figures 21 and 22, where it can be seen that increasing the amount of residue increases the amount of particles emitted. The distribution of the particles is not influenced much and the peak concentrations of mass and number of particles are at similar particle sizes. Figures 23 and 24 show that the same is true for the 10 % load case. The distribution approximately retains its form but the amount of particles and mass is increased throughout the range.
The reasons for higher emissions with increased residue are logical. Firstly the residue is the component from which the polymer forming the cenosphere is created and so more of the residue component directly leads to production of more polymer. Secondly increasing the amount of residue makes the fuel burn poorer decreasing temperatures in the cylinder and thus possibly slowing down the burnout of cenospheres.

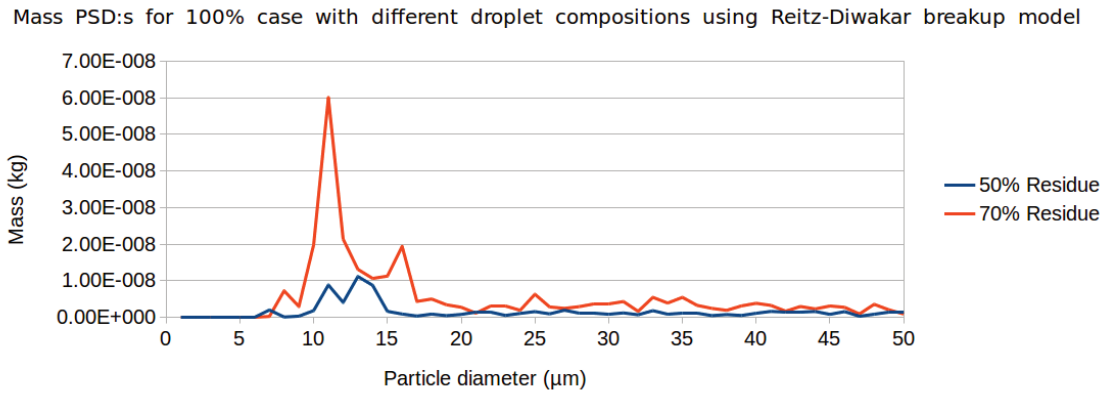

Figure 21: The particle mass-size distributions produced by different fuel compositions with Reitz-Diwakar breakup regime

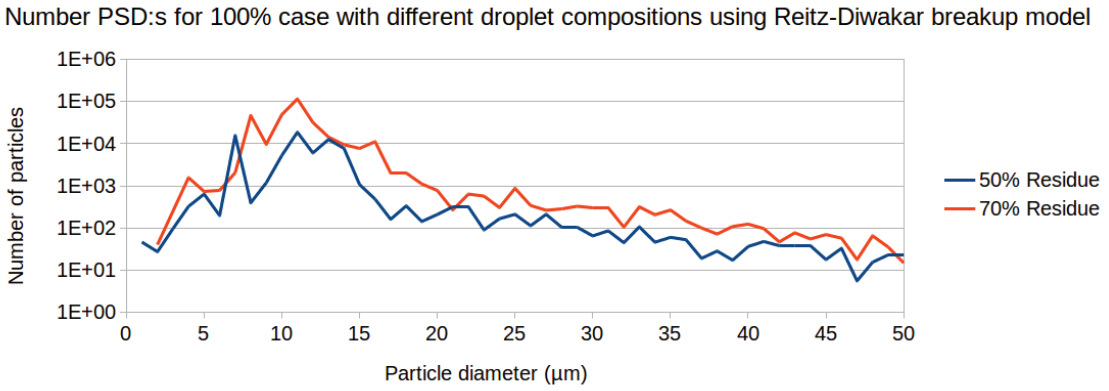

Figure 22: The particle number-size distributions produced by different fuel compositions with Reitz-Diwakar breakup regime

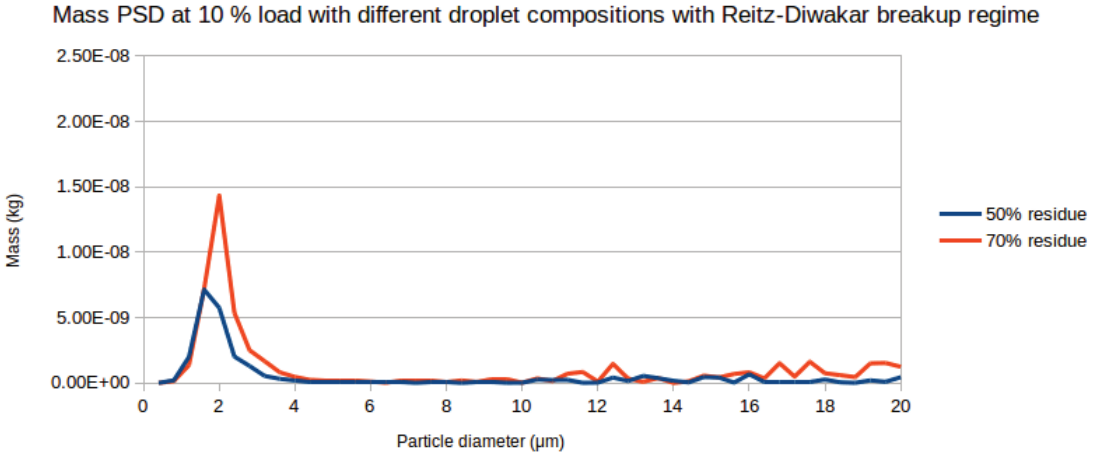

Figure 23: The particle mass-size distributions produced by different fuel compositions for 10 % load case with Reitz-Diwakar breakup regime

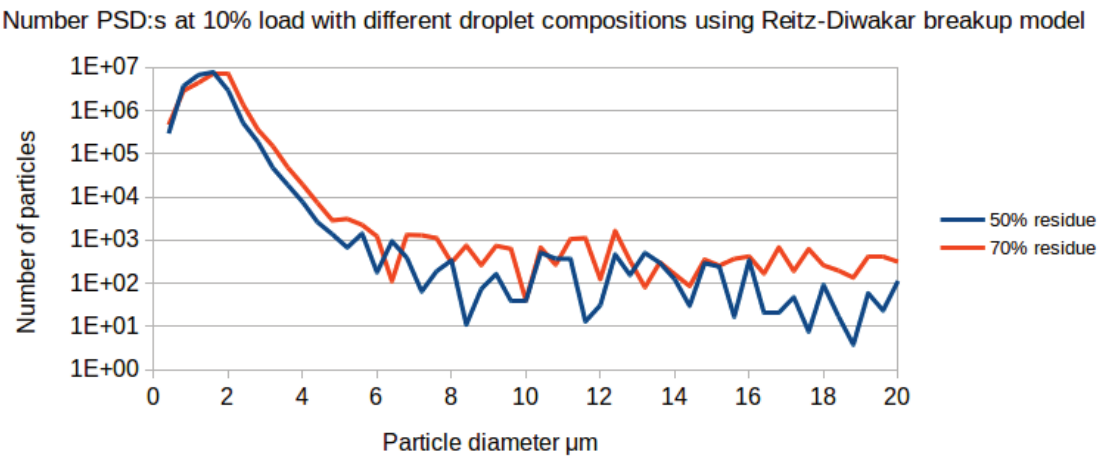

Figure 24: The particle number-size distributions for 10 % load case produced by different fuel compositions with Reitz-Diwakar breakup regime

4.3 Conclusions

The value of a CFD model is in the conclusions that can be drawn from the results it produces. Therefore the results presented previously are interpreted in this section and the conclusions are evaluated against what is known about the different phenomena from literature. The main conclusions that can be drawn from this model about the behaviour of cenosphere emissions from a diesel engine using HFO are as follows:

1. Size distribution of emitted cenospheres has a correlation to the size distribution of fuel droplets.

2. Increasing the load at same speed (RPM) will decrease the cenosphere emissions relative to fuel consumption.

3. Cenospheres of widely varying sizes are found in emissions and size distributions of cenospheres emitted are dependent on load. At lower loads highest amount of particles are found with a diameter of less than 2 μm while at full load the peak concentration of particles is around 10 μm.

4. Improving atomization of spray will decrease emitted particle mass but may still increase number of emitted particles.

5. Higher viscosity leads to larger particles.

6. Increasing the amount of heavy components in the fuel increases emissions of cenospheres of all sizes.

7. A well working atomization model is important for accurate results

That the size distributions of emitted cenospheres have a correlation to the size distributions of fuel droplets is not surprising as every droplet forms a cenosphere in the present model. The assumption of every droplet forming a cenosphere is supported by the findings of Bomo et al. and could thus be concidered reasonable[13]. Bartle et al. also reported a strong similarity between droplet size distributions in the fuel spray and resulting cenosphere emissions[41]. The finding that influencing droplet size distributions influences cenosphere sizes would indicate that emissions of cenospheres could conceivably be influenced by modifying spray atomization.

Indeed it was found that improving atomization will decrease emissions of cenospheres, at least in terms of mass of cenospheres emitted. The finding is not surprising as smaller particles would take less time to burn out, and as burnout of particles is improved, the emissions are naturally lowered. The conclusion that improved atomization will decrease the emissions of particulate mass was also drawn by the modeling studies of Baert and Youan[14][24]. The finding that decreasing the size of the droplets often seem to lead to an increased number of droplets emitted could be a factor to consider if the number of cenospheres, rather than the mass of cenospheres, is of particular concern.

Increasing the viscosity of the fuel increases both the sizes of droplets and the resulting cenospheres. This is not surprising concidering the formulations of the droplet breakup models and is also consistent with experimental findings in literature[41]. As the viscosity of the droplets influences atomization, and consequently cenosphere emissions, taking viscosity into account in a reasonable way is important in the present context. Generally viscosity has a tendency to decrease with increased temperature and there are multicomponent evaporation models that model viscosity as a function of temperature available for HFO combustion in context of marine diesel engines[17]. However, as noted by Goldsworthy the preferential evaporation of lighter components will counteract the tendency for viscosity to decrease with temperature due to the highly viscous nature of the residue[15]. Therefore the present models use of Goldsworthy's assumption of constant viscosity is not completely unreasonable. A model in which viscosity is modelled as a function of both fuel composition and temperature could provide even more accurate results regarding the behaviour of the droplets, compared to the assumption of constant viscosity.
Changing the fuel composition by increasing the share of the residue component in the fuel increases the emissions of cenospheres of all sizes. As discussed earlier this was to be expected and it also agrees with studies in literature which state that poorer quality fuels produce more coke emissions[18][41]. Here the effect of increasing the residue part was studied in an isolated manner without it affecting other fuel properties. In reality increasing the share of residue would affect the viscosity of the droplet and thus the effect on cenosphere emissions could be even more pronounced than observed here[41].
The fact that the emissions relative to injected fuel are diminished as load increases is supported by much data found on emissions from engines in literature. For instance Sarvi et al. observed better burnout of carbon at high loads. [40] Also the higher number concentrations of PM in the 10% in absolute terms compared to the full load case could be consistent with the FSN trend that was available in the experimental data available for the cases. Both the peak concentration of mass at particle sizes of around 10 μm in diameter for the 100 % case and the presence of particles of a wide range of sizes could be considered consistent with the findings of Lyyränen et al.[11].

Although the present model does seem to react in reasonable manner according to the results presented above, it is difficult to conclusively validate the performance of the model without more detailed measurement data from the specific case studied here. Accurate measurement data about cenosphere emissions from engines in particular and their dependence on factors such as load would be necessary for accurate calibration of the present model. As such detailed data is not available for the present case, or similar cases in the literature, this study is limited to assessing the performance of the present model through the way the results react to different changes in the simulation, rather than focusing on the specific emission levels. Even if there may be some uncertainty when it comes to the exact emission levels predicted by this model it may however still provide useful information about the formation of these emissions, and the way these emissions are impacted by changes in different operating conditions.

5 Recommendations for future work

One of the challenges faced in this work was the incompatibility of the present model with the droplet collision models and the standard solution procedure for lagrangian flow in Star CD. Further development of the model to amend these compatibility issues would be useful for getting more reliable and accurate results. This was however not possible within the scope of this thesis. As discussed earlier a more detailed approach to model the viscosity of the droplet could be beneficial, especially when using the model for cenosphere emissions modelling. Additionally, while this work attempts to prove the possibilities of this modelling approach, a experimental case for which detailed data about both fuel and the cenosphere emissions is available would be useful for more conclusive validation of the model.

The multicomponent continuous thermodynamics approach to modelling fuel droplet properties and behaviour used in this work could also be used in other applications than PM emissions modelling. Exploring the opportunities presented by the approach for engine combustion in a general sense could prove useful. Especially in cases where the fuel composition is such that a single component model for the fuel proves insufficient to capture the evaporation behaviour of the fuel, the present model could provide useful tools for fine-tuning the behaviour of the fuel.

References

[1] D. Argyros, N. Sabio, C. Raucci, and T. Smith, "Global marine fuel trends 2030," tech. rep., Lloyd's Register Group Limited, UCL Energy Institute, 2014.

[2] I. Bennett, "Heavy fuel oil combustion; a market segmentation report," tech. rep., TBD Presentations, 2011.

[3] V. Garaniya, *Modelling of Heavy Fuel Oil Spray Combustion Using Continuous Thermodynamics*. PhD thesis, University of tasmania, 2009.

[4] M. . Bahls, "Important terms from a to z:heavy fuel oil (hfo)," 2015.

[5] Marpol, "Marpol annex i: Regulations for the prevention of pollution by oil," 1983.

[6] ISO, "Iso 8217:2012(en) petroleum products — fuels (class f) — specifications of marine fuels," tech. rep., International Organisation for standards, 2012.

[7] M. B. Vermeire, "Everything you need to know about marine fuels," tech. rep., Chevron Global Marine Products, 2012.

[8] ABS, "Notes on heavy fuel oil," tech. rep., American Bureaou of Shipping, 1984.

[9] R. C. Flagan, *Chapter 6 – Particle Formation in Combustion*. 1988.

[10] A. Kasper, S. Aufdenblatten, A. Forss, and H. B. M. Mohr, "Particulate emissions from a low-speed marine diesel engine," *Aerosol Science and Technology*, 2007.

[11] J. Lyyränen, J. Jokiniemi, E. I. Kauppinen, and J. Joutsensaari, "Aerosol characterisation in medium-speed diesel engines operating with heavy fuel oils," *Journal of Aerosol Science*, 1999.

[12] "Distinctive combustion stages of single heavy oil droplet under microgravity," *Fuel*, vol. 82, no. 3, pp. 293 – 304, 2003.

[13] N. Bomo, J. Lahaye, G. Prado, and G. Claus, "Twentieth symposium (international) on combustion formation of cenospheres during pyrolysis of residual fuel oils," *Symposium (International) on Combustion*, vol. 20, no. 1, pp. 903 – 911, 1985.

[14] R. Baert, "A mathematical model for heavy fuel droplet vaporization and pyrolysis in a high temperature inert gas," *Combustion Science and Technology*, 1993.

[15] L. Goldsworthy, "Computational fluid dynamics modelling of residual fuel oil combustion in the context of marine diesel engines," *International Journal of Engine Research*, 2006.

[16] D. Struckmeier, D. Tsuru, S. Kawauchi, and H. Tajima, "Multi-component modeling of evaporation, ignition and combustion processes of heavy residual fuel oil," *SAE Technical Paper 2009-01-2677*, 2009.

[17] N. Kyriakides, C. Chryssakis, and L. Kaiktsis, "Influence of heavy fuel properties on spray atomization for marine diesel engine applications," *SAE Technical Paper 2009-01-1858*, 2009.

[18] H. L. Goldstein and C. W. Siegmund, "Influence of heavy fuel oil composition and boiler combustion conditions on particulate emissions," *Environmental Science Technology*, 1976.

[19] N. J. Marrone, I. M. Kennedy, and F. L. Dryer, "Coke formation in the combustion of isolated heavy oil droplets," *Combustion Science and Technology*, 1984.

[20] H. Omidvarborna, A. Kumar, and D.-S. Kim, "Recent studies on soot modeling for diesel combustion," *Renewable and Sustainable Energy Reviews*, 2015.

[21] P. Antaki, "Transient processes in a rigid slurry droplet during liquid vaporization and combus- tion," *Combustion Science Technology*, 1986.

[22] A. Lee and C. Law, "Gasification and shell characteristics in slurry droplet burning," *Combust. Flame*, 1991.

[23] L. W. P. Moszkowicz and G. Claus, "Modelling of very fast pyrolysis of heavy fuel oil droplets," *Chem. Eng. Sci*, 1996.

[24] J. Yuan, V. Semiao, and M. G. Carvalho, "Modelling and validation of the formation and oxidation of cenospheres in a confined spray flame," *International Journal of Energy Research*, 1997.

[25] V. M. Reddy, M. M. Rahman, A. N. Gandi, A. M. Elbaz, R. A. Schrecengost, and W. L. Roberts, "Cenosphere formation from heavy fuel oil: a numerical analysis accounting for the balance between porous shells and internal pressure," *Combustion Theory and Modelling*, vol. 20, no. 1, pp. 154–172, 2016.

[26] C. Fink, B. Buchholz, M. Niendorf, and H. Harndorf, "Injection spray analyses from medium speed engines using marine fuels," *ILASS*, 2008.

[27] D. L. Urban, S. P. Huey, and F. L. Dryer, "Evaluation of the coke formation potential of residual fuel oils," *Symposium (International) on Combustion*, 1992.

[28] CIMAC, "Background information on black carbon emissions from large marine and stationary diesel engines - definition, measurement methods, emission factors and abatement technologies," tech. rep., CIMAC, 2012.

[29] WHO, "Health effects of particulate matter," tech. rep., World Health Organisation, 2013.

[30] N. Janssen, P. Fischer, M. Marra, C. Ameling, and F. Cassee, "Short-term effects of pm2.5, pm10 and pm2.5–10 on daily mortality in the netherlands," *Science of The Total Environment*, 2013.

[31] J. S. Lighty, J. M. Veranth, and A. F. Sarofim, "Combustion aerosols: Factors governing their size and composition and implications to human health," *Journal of the Air Waste Management Association*, 2000.

[32] O. Kaario, *The Infuence of Certain Submodels on Diesel Engine Modeling Results*. PhD thesis, Helsinki University of technology, Department of Mechanical Engineering, 2007.

[33] J. Abraham, F. Bracco, and R. Reitz, "Comparisons of computed and measured premixed charge engine combustion," *Combustion and Flame*, 1985.

[34] S.-C. Kong and R. D. Reitz, "Multidimensional modeling of diesel ignition and combustion using a multistep kinetics model," *Journal of Engineering for Gas Turbines and Power*, 1993.

[35] *METHODOLOGY-STAR CD® VERSION 4.24*.

[36] C. H. Bong, *Numerical and Experimental Analysis of Diesel Spray Dynamics including the Effects of Fuel Viscosity*. PhD thesis, University of Tasmania, 2010.

[37] J. Moldanova, E. Fridell, O. Popovicheva, B. Demirdjian, V. Tishkova, A. Faccinetto, and C. Focsa, "Characterisation of particulate matter and gaseous emissions from a large ship diesel engine," *Atmospheric Environment*, 2009.

[38] J. Lyyränen, J. Jokiniemi, and E. Kauppinen, "The effect of mg-based additive on aerosol characteristics in medium-speed diesel engines operating with residual fuel oils," *Journal of Aerosol Science*, 2002.

[39] E. Fridell, E. Steen, and K. Peterson, "Primary particles in ship emissions," *Atmospheric Environment*, vol. 42, no. 6, pp. 1160 – 1168, 2008.

[40] A. Sarvi, J. Lyyränen, J. Jokiniemi, and R. Zevenhoven, "Particulate emissions from large-scale medium-speed diesel engines: 2. chemical composition," *Fuel Processing Technology*, 2011.

[41] K. Bartle, J. Jones, A. Lea-Langton, M. Pourkashanian, A. Ross, J. Thillaimuthu, P. Waller, and A. Williams, "The combustion of droplets of high-asphaltene heavy oils," *Fuel*, vol. 103, pp. 835 – 842, 2013.

[42] R. Villasenor and F. Garcia, "An experimental study of the effects of asphaltenes on heavy fuel oil droplet combustion," *Fuel*, 1999.